



HAL
open science

Insights in aroma compound retention by mucosa during consumption through mathematical modelling

Isabelle Deleris, Anne Saint-Eve, Aurélie Saglio, Isabelle Souchon,
Ioan-Cristian Trelea

► To cite this version:

Isabelle Deleris, Anne Saint-Eve, Aurélie Saglio, Isabelle Souchon, Ioan-Cristian Trelea. Insights in aroma compound retention by mucosa during consumption through mathematical modelling. *Journal of Food Engineering*, 2016, 190, pp.123-138. 10.1016/j.jfoodeng.2016.06.018 . hal-01532599

HAL Id: hal-01532599

<https://hal.science/hal-01532599>

Submitted on 11 Jul 2017

HAL is a multi-disciplinary open access archive for the deposit and dissemination of scientific research documents, whether they are published or not. The documents may come from teaching and research institutions in France or abroad, or from public or private research centers.

L'archive ouverte pluridisciplinaire **HAL**, est destinée au dépôt et à la diffusion de documents scientifiques de niveau recherche, publiés ou non, émanant des établissements d'enseignement et de recherche français ou étrangers, des laboratoires publics ou privés.

1 **INSIGHTS IN AROMA COMPOUND RETENTION BY MUCOSA DURING**
2 **CONSUMPTION THROUGH MATHEMATICAL MODELLING**

3 **Isabelle Déléris, Anne Saint-Eve, Aurélie Saglio, Isabelle Souchon, Ioan Cristian Trelea**

4 UMR 782 GMPA, AgroParisTech, INRA, Université Paris-Saclay, 78850, Thiverval-
5 Grignon, France

6 isabelle.deleris@grignon.inra.fr; seanne@grignon.inra.fr; isabelle.souchon@grignon.inra.fr;

7 cristian.trelea@agroparistech.fr

8 *Correspondence to be sent to: Isabelle Déléris, UMR 782 Génie et Microbiologie des*
9 *Procédés Alimentaires, 1 avenue Lucien Brétignières, F-78850 Thiverval-Grignon, France.*

10 *email: isabelle.deleris@grignon.inra.fr*

Highlights

- Aroma compound persistence after gaseous sample inhalation was modelled.
- Both physiological and physicochemical parameters were included in the model.
- The respective contributions of wetted mucosa and saliva on release kinetics were assessed.
- The major role of mucosa partition coefficients of molecules was confirmed.

11 **Abstract**

12 A multidisciplinary approach combining physiology and physical chemistry and associating
13 experimental measurements with *in silico* modelling was applied to explain the release of
14 aroma compounds during food consumption. Experimental release kinetics obtained by
15 inhaling gaseous samples through controlled protocols highlighted different release
16 behaviours, depending on aroma compound properties. The associated mathematical model
17 described mass transfer mechanisms between the different compartments of the naso-oro-
18 pharyngeal cavities and included both physicochemical and physiological parameters. One of
19 the main developments was notably to consider the possible retention of aroma compounds by
20 wetted mucosa. **Model sensitivity analysis confirmed the key role of interaction between**
21 **aroma compounds and mucosa (air/mucosa partition coefficient) and of individual breath**
22 **parameters (current breath volume and respiratory frequency) on the persistence of aroma**
23 **compound in exhaled air.** These achievements show that the association of an experimental
24 approach and mechanistic modelling constitutes a powerful tool to improve the understanding
25 of aroma release and persistence.

26 **Keywords:** aroma release, wetted mucosa, saliva, persistence, interaction, dynamic modelling

27 **Chemical compounds studied in this article:**

28 ethyl propanoate (PubChem CID: 7749), 2-nonanone (PubChem CID: 13187), (Z)-3-hexen-1-
29 ol (PubChem CID: 10993), polypropylene glycol (PubChem CID: 1030).

30 **Short running title:** Modelling of *in vivo* aroma retention

31 **Highlights**

- 32 - Aroma compound persistence after gaseous sample inhalation was modelled.
- 33 - Both physiological and physicochemical parameters were included in the model.
- 34 - The respective contributions of wetted mucosa and saliva on release kinetics were assessed.
- 35 - The major role of mucosa partition coefficients of molecules was confirmed.

36 1. Introduction

37 Olfactory perception is known to largely contribute to overall perception of foods and,
38 consequently, to consumer choice and preferences. A better understanding of this specific
39 perception is therefore of great importance and requires the identification of the main
40 mechanisms at the origin of aroma compound release during food consumption. Several
41 studies have notably focused on orthonasal and retronasal perceptions to highlight the origin
42 of the main differences between these two perception pathways (Espinosa Diaz, 2004;
43 Halpern, 2004; Heilman and Hummel, 2004; Hummel, 2008; Hummel *et al.*, 2006; Sun and
44 Halpern, 2005; Visschers *et al.*, 2006; Welge-Lüssen *et al.*, 2009). The large number and the
45 variety of mechanisms (physical, chemical, physiological, neurobiological, cognitive, *etc.*)
46 that can be involved at different space and time scales largely contribute to the complexity of
47 perception. Among them, the release dynamics of aroma compounds have long been known to
48 be among key factors to explain aromatic perceptions (Barron *et al.*, 2012; Biasioli *et al.*,
49 2006; Déléris *et al.*, 2011; Gierczynski *et al.*, 2011; Heenan *et al.*, 2009). Numerous studies in
50 the literature have focused on the identification of the main factors that can impact release
51 kinetics, either related to the physicochemical properties of the molecules, to product
52 characteristics (composition, structure), to individual physiology (saliva composition and flow
53 rate, breath flow rate) or to oral processing (chewing efficiency, product coating, *etc.*)
54 (Benjamin *et al.*, 2012; Buettner and Beauchamp, 2010; Foster *et al.*, 2011; Frank *et al.*, 2012;
55 Gierczynski *et al.*, 2011; Heath, 2002; Heenan *et al.*, 2011). The existence of aroma
56 compound retention by wetted mucosa has often been proposed to explain specific release
57 behaviours, but little is known about the origin of this phenomenon. However, several
58 mechanisms have been suggested in the literature: the interaction of aroma compounds with
59 the constituents of the mucus layer (mucins, enzymes, antioxidants, ionic compounds), with
60 saliva and/or with the mucosa tissues themselves (Buettner and Beauchamp, 2010); the role of

61 the contact area between nasal mucus and air (Keyhani *et al.*, 1997); the role of the
62 physicochemical properties of aroma compounds (Ferreira *et al.*, 2006; Tromelin *et al.*, 2010);
63 and the role of breath and/or salivary flow rates (Buettner and Mestres, 2005; Hodgson *et al.*,
64 2004).

65 Performing *in vivo* experiments and developing appropriate experimental set-ups constitute
66 the main difficulties involved in exploring this topic and in validating or not the assumptions.

67 A previous study proposed various simple protocols to explore and quantify *in vivo* aroma
68 release and persistence from gaseous samples, depending on the exposed physiological
69 cavities (nose, mouth or pharynx) (Dél ris *et al.*, 2015). Results confirmed the main role of
70 aroma compound properties and highlighted the possible occurrence of different types of
71 mechanisms, either physical or biochemical, to explain release behaviours. The global nature
72 of the approach and the complexity of the phenomena involved did not allow the authors to
73 clearly identify the relative contribution of each mechanism.

74 The difficulty of dissociating all of the phenomena that occur during *in vivo* experiments
75 generally prevents from determining the respective contribution of product properties or of
76 consumer characteristics to aroma release. Due to these experimental issues, the modelling
77 approach (*in silico*) can be a useful tool to improve the understanding. It has been largely used
78 in the fields of pharmacokinetics and toxicology: Quantitative Structure-Activity
79 Relationships (QSAR) (Geerts and Heyden, 2011), Physiologically-Based Pharmaco-Kinetic
80 (PB-PK) (Corley *et al.*, 2012; Medinsky *et al.*, 1993; Morris, 2012) and Theoretical Passive
81 Absorption (TPAM) (Obata *et al.*, 2005; Takano *et al.*, 2006) models have helped to better
82 understand drug and toxic vapour absorption. In the field of olfaction, the QSAR approach
83 has also been largely used to identify the main interactions between aroma compounds and
84 olfactory receptors at the origin of perception (Anker *et al.*, 1990; Chastrette and Rallet, 1998;
85 Kraft *et al.*, 2000; Rognon and Chastrette, 1994; Sanz *et al.*, 2008). Some of these models

86 clearly highlighted the need to consider absorption/solubilisation phenomena in tissues of the
87 respiratory tract and/or in the mucus layer to correctly represent the availability of aroma
88 compounds for olfactory receptors. It was demonstrated that the transport of odorant
89 molecules in nasal mucosa clearly differs from the one within an aqueous layer (Kurtz *et al.*,
90 2004). The main limitation of modelling approaches remains the lack of experimental data,
91 notably concerning the air/mucosa partition or diffusion properties of aroma compounds
92 within the mucus layer, or mucosa characteristics depending on its location (nasal, oral or
93 pharyngeal cavity).

94 In food science, some mechanistic models describing volatile release have been proposed and
95 sometimes compared to experimental *in vivo* data (Buffo *et al.*, 2005; Harrison, 2000;
96 Harrison and Hills, 1997; Hodgson *et al.*, 2005; Normand *et al.*, 2004; Wright and Hills,
97 2003). These models, based on physical, chemical and physiological parameters, led to more
98 or less good predictions of the release kinetics of aroma compounds, but only for liquid food
99 products. Only the models of (Wright and Hills, 2003) and (Normand *et al.*, 2004) included a
100 term representing possible interactions between aroma compounds and mucosa and/or
101 salivary constituents. Even though many publications exist on molecular mechanisms that
102 explain interactions between aroma compounds and proteins in the mucus of the nasal cavity
103 of rats (Odorant Binding Proteins, OBPs), results cannot be directly used to explain *in vivo*
104 release kinetics in humans (Borysik *et al.*, 2010; Yabuki *et al.*, 2011). All of these studies
105 constitute a first step in describing the phenomena involved but do not yet provide a clear
106 understanding. In a previous publication, a mathematical model was proposed to predict *in*
107 *vivo* aroma release from masticated food products that considered food properties and the
108 physiological characteristics of the individuals (Doyennette *et al.*, 2014). Comparison
109 between experimental and predicted kinetics highlighted the possible specific retention of one
110 hydrophobic aroma compound by wetted mucosa and mucus in the naso-oro-pharyngeal

111 cavities. This model thus needs to be further developed to propose a satisfactory quantitative
112 description of the retention phenomenon at the origin of aroma persistence.

113 In this context, the main goal of the present study is to better understand the mechanisms
114 underlying aroma release and persistence. The originality of the proposed approach is to
115 combine: (i) *in vivo* aroma release measurements (using controlled protocols to ensure aroma
116 supply by flavoured air inhalation, without the interference of any food product); with (ii) the
117 detailed mechanistic modelling of mass transfer to investigate the key mechanisms
118 responsible for the release profiles and/or retention of aroma compounds.

119 2. Material and methods

120 Even if this study was not performed in the field of medical research, a detailed research
121 protocol containing the relevant information in agreement with the World Medical
122 Association Declaration of Helsinki was done. Only single-use materials were used with
123 panellists. Aroma compounds were all food grade and their liquid concentrations were
124 adjusted to limit gaseous concentration and ensure panellist comfort and avoid sensory
125 saturation. Only one session (45 minutes) per week was planned for each panellist and the
126 number of samples during one session was limited to five. Samples were coded to protect the
127 privacy of panellist and the confidentiality of their personal information. Subjects were clearly
128 informed of the observational nature of this study, gave their free and informed consent and
129 received compensation for their participation.

130 2.1. Aroma compounds

131 Food grade quality aroma compounds (ethyl propanoate, 2-nonanone and (*Z*)-3-hexen-1-ol)
132 were purchased from Sigma Aldrich (France) (Table 1).

133 They were selected since they belong to several chemical classes and present different
134 physicochemical properties and different release behaviours in terms of persistence (Déléris *et*
135 *al.*, 2015). Concentrated stock solutions were prepared in polypropylene glycol (Sigma

136 Aldrich, France) and used throughout the study. Diluted solutions were prepared
137 extemporaneously.

138 2.2. Gaseous sample preparation

139 An aroma compound mixture was used to reduce the number of experimental sessions.
140 Gaseous samples were prepared as previously described (Déléris *et al.*, 2015). The
141 concentrations of aroma compounds in the liquid phase were high enough to be detected
142 during PTR-MS measurements, while being acceptable from a sensory point of view for the
143 panellists: 1000 mg/kg for (Z)-3-hexen-1-ol, 150 mg/kg for ethyl propanoate and 100 mg/kg
144 for 2-nonanone.

145 Twenty-five mL of flavoured aqueous solution were stored at ambient temperature for 4 hours
146 before measurements in 250-mL flasks (Schott, France), closed by caps equipped with valves
147 (equilibrium establishment). To control the inhaled volume of gaseous sample (and, therefore,
148 the amount of inhaled aroma compounds) between the different assays, a specific set-up was
149 developed to prepare gaseous samples (Figure 1): a manual pump was connected to one of the
150 cap valves and used to push some fresh air into the flasks. By way of this procedure,
151 flavoured air was introduced into a balloon positioned on the other valve of the flask cap.
152 Three pump strokes were needed to prepare 200 mL of gaseous sample, which was considered
153 as appropriate to be inhaled by panellists in one breath. Once inflated, balloons were closed
154 with plastic pliers.

155 The study of the variation of aroma concentration within balloons during storage highlighted
156 the fact that this preparation had to be done less than 30 s before measurement to avoid any
157 loss of aroma compounds (not shown). Even if some interactions between aroma compounds
158 and balloon material could occur, they were assumed to always be the same and to not
159 influence the results since all conditions were controlled.

160 2.3. Panellists

161 Eight panellists (four men and four women, 22-45 years old) were recruited for the study.
162 They were instructed not to smoke, eat, drink or use any persistent-flavoured product for at
163 least one hour before Proton Transfer Reaction-Mass Spectrometry (PTR-MS) or saliva
164 collection sessions.

165 When dealing with aroma release and food oral processing, lots of studies in literature largely
166 highlighted the key role that anatomy and physiology can have on the dynamics of
167 phenomena (Buettner and Beauchamp, 2010; Féron *et al.*, 2014; Foster *et al.*, 2011; Repoux *et*
168 *al.*, 2012b). Some physiological measurements were thus performed on panellists who
169 participated to this study to define the range of variation of these parameters for the panel.

170 The volumes of the oral, nasal and pharyngeal cavities of the subjects were measured with the
171 Eccovision Acoustic Rhinopharyngometer (Sleep Group Solutions, North Miami Beach, FL,
172 USA). Software was developed to automatically calculate the air/product areas of the oral and
173 pharyngeal cavities for each individual (Doyennette *et al.*, 2011). The tidal volume of each
174 individual was measured with a spirometer (Pulmo System II, MSR, Rungis, France) (Repoux
175 *et al.*, 2012a).

176 Non-stimulated saliva was collected by asking volunteers to swallow the saliva in their mouth
177 before starting and to then spit each 30 s for 5 min into ice-chilled vessels. The final saliva
178 weight was measured and the flow rate was calculated as g/min. Whole saliva samples were
179 centrifuged at 13400×g for 5 min at 4°C to remove cellular debris (Eppendorf, model 5415 R,
180 Germany). The supernatants were frozen and stored at -80°C before analysis. Protein
181 concentration (expressed in mg/mL) was obtained by standard Bradford protein assay Quick
182 Start (Bio-Rad, France) using bovine serum albumin (Sigma-Aldrich, France) as the standard
183 calibration. The lipolytic (lipolysis), proteolytic (proteolysis), lysozymal (lysozyme) and
184 amylolytic (amylase) activities of individual salivas (expressed in U/mL) were determined as
185 previously described (Neyraud *et al.*, 2012).

186 Three replicates per physiological parameter and per panellist were performed. The minimal,
187 median and maximal values of physiological characteristics and associated quartiles are
188 summarized in Table 2.

189 2.4. Determination of aroma *in vivo* release kinetics using PTR-MS measurements

190 Release kinetics were obtained using the reference protocol previously defined (referred to as
191 the Nose, Mouth, Swallowing protocol, or N.M.S.) (Déléris *et al.*, 2015): sample inhalation
192 was performed through the panellist's mouth in one short breath and the measurement of
193 aroma release was made within the panellist's nasal cavity.

194 During a session, subjects started with the analysis of a blank sample to get used to the
195 protocol and then tested five samples. The measurement procedure was similar to the one
196 previously described (Déléris *et al.*, 2015): room and breath analyses for 10 s and 30 s,
197 respectively, followed by sample inhalation and release measurement. During the assay,
198 panellists were allowed to swallow. Between each sample, panellists cleaned their mouth with
199 mineral water (Evian, Danone) and their breath was retested before each new measurement.

200 Some differences with the previous study should be mentioned. First, swallowing events were
201 imposed: 20 s after sample inhalation for the first swallow, and then every 30 s until the end
202 of measurement. Secondly, the sample volume was standardised, allowing the quantitative
203 comparison between protocols. Three sessions of 45 min were planned to obtain three
204 replicates of the five samples for each subject. All the measurements were performed within a
205 21-day period.

206 The High-Sensitivity Proton Transfer Reaction-Mass Spectrometer (PTR-MS) (Ionicon
207 Analytik, Innsbruck, Austria) was operated at a drift tube temperature, voltage and pressure of
208 60°C, 600.1 (± 0.4) V and 2.0 (± 0.01) mbar, respectively ($E/N=151.4 (\pm 1.4)$ Td). Nose-space
209 was sampled *via* two inlets of a stainless nosepiece placed in both nostrils of the assessors.
210 The inlet of the PTR-MS instrument was connected to the sampling device *via* a 1/16"

211 PEEKTM tube maintained at 110°C. Measurements were performed using the Multiple Ion
212 Detection (MID) mode. For a mass/charge ratio (m/z) of 21 (H_3O^+) and 37 ($\text{H}_2\text{O}-\text{H}_3\text{O}^+$), the
213 dwell time per mass was fixed to 0.05 s. The mean signal for H_3O^+ was $7.8 \times 10^6 \pm 0.8 \times 10^6$
214 counts per second (cps) and its day-to-day variation along the measurement period was 10%.
215 The signal for $\text{H}_2\text{O}-\text{H}_3\text{O}^+$ did not exceed 4% of the one of m/z 21 (in agreement with
216 equipment specifications).

217 Using the fragmentation patterns of individual compounds (Table 1), the molecules studied
218 were monitored at m/z 83 ((*Z*)-3-hexen-1-ol), m/z 75 and 103 (ethyl propanoate) and m/z 143
219 (2-nonanone). For these four specific masses, a dwell time per mass of 0.1 s was selected as a
220 compromise between sensitivity for aroma compound detection and appropriate sampling
221 frequency with regard to phenomena to be measured. In addition, m/z 59 and 93 were
222 monitored with a dwell time per mass of 0.05 s as markers of panellists' breath (Weel *et al.*,
223 2002) and of balloon material, respectively. With these settings, exhaled air was sampled
224 every 0.6 s, which was assumed to be appropriate regarding the mean duration of the
225 breathing cycle (Doyennette *et al.*, 2011; Sherwood, 2006; Tortora and Anagnostakos, 1990).
226 Mean signal-to-noise ratios varied between 2.0 and 38.0 (depending on the ions), meaning
227 that responses during sample analysis sufficiently exceeded the baseline. These measurements
228 led to the determination of molecule release kinetics, *i.e.*, intensity $I_t = f(\text{time } t)$, for each
229 panellist. Since solution composition was precisely known, aroma compounds were
230 unambiguously detected at the stated m/z ratio. For this reason and to facilitate text
231 readability, compound names rather than their m/z ratio are used hereafter.

232 For data handling, experimental release curves were divided into three main periods: (i) the
233 phase before the product was inhaled (phase 0); (ii) the phase before the first swallow (phase
234 1); and (iii) the phase after the first swallow (phase 2). For each sample, the mean PTR-MS
235 signal measured during phase 0 was subtracted from the PTR-MS signals obtained during

236 phases 1 and 2. Some quantitative release parameters were extracted from each individual
237 release curve and for each phase of product consumption: maximal intensities ($I_{\max 1}$ and
238 $I_{\max 2}$), which indicate the maximum concentration reached by a compound; and areas under
239 the curve (AUC_1 and AUC_2), which are related to the total amount of molecule that is
240 released). The ratios between areas under the curve before and after swallowing were also
241 calculated (AUC_1/AUC_2). Some temporal release parameters such as times at which I_{\max}
242 occurred ($t_{\max 1}$ and $t_{\max 2}$) and initial release rates ($Rate_1$ and $Rate_2$, calculated by dividing the
243 I_{\max} values with the t_{\max} times) were also determined. Peak widths for each phase were
244 obtained as the difference between the two times at which the intensity was 20% of I_{\max} (after
245 and before release peak) ($\Delta t_{20\%_1}$ and $\Delta t_{20\%_2}$). The difference between the time at which the
246 intensity was 50% of I_{\max} after the peak and t_{\max} ($t_{50\%}-t_{\max}$) was also extracted. In addition,
247 standardised release kinetics were obtained by dividing each intensity value of the curve by
248 the corresponding I_{\max} ($I_{t_stand}=I_t/I_{\max}$). Standardised areas under the curve ($AUC_{stand.}$),
249 determined from these standardised kinetics, were used as an indication of persistence
250 behaviour. Because the objective was to compare the persistence of aroma release between
251 molecules, the use of arbitrary units for aroma concentration data was sufficient for data
252 analysis. Since the two ions related to ethyl propanoate behaved in the same way, only the
253 result of m/z 75 is presented in the text.

254 Non-parametric descriptive analysis was carried out on datasets and comparative analysis was
255 performed using Kruskal-Wallis tests and the Conover-Iman procedure (multiple paired
256 comparisons) to highlight differences in *in vivo* release kinetics between molecules. The level
257 of significance was set at $p<0.05$.

258 3. Modelling

259 3.1. Principles of the model

260 The aroma release model presented in this study was developed to describe aroma release
261 after one inhalation of a gaseous sample through the mouth. It is based on equations that
262 describe mass transfers that occur between the different physiological cavities (mouth, nose,
263 pharynx), considered as interconnected reactors that vary in volume and that exchange
264 matter.

265 A schematic representation of the four physiological cavities involved in the model design, as
266 well as their connections and the mechanisms responsible for aroma release, are given in
267 Figure 2. A schematic representation of mass transfer between air, saliva and mucosa within a
268 physiological cavity is presented in Figure 3. All variables and parameters required for the
269 model simulation are specified in these figures and described in Tables 3 and 4, respectively.

270 The model describes the steps of the experimental protocol: sample inhalation through the
271 mouth, exposure period to the sample until the first swallow, and post-swallow release.
272 Except for the first inhalation, breathing occurs through the nose. Each swallowing step is
273 known to be very short (Martin-Harris, 2006) compared to persistence phenomena (Hodgson
274 *et al.*, 2004; Normand *et al.*, 2004). Swallowing events are thus described as quick
275 simultaneous contractions of the oral cavity and of the pharynx, leading to air expulsion,
276 followed by relaxation and filling with fresh air (Doyennette *et al.*, 2014).

277 Two compartments in the mouth and in the pharynx (mucosa and saliva) and one
278 compartment in the nose (mucosa) were included in the model to introduce a reservoir effect
279 (Figure 2). In each cavity, the air phase was assumed to be in contact with mucosa and/or
280 saliva layers. The proportions of these contact areas can be changed in the model to evaluate
281 the respective contributions of saliva and mucosa. The volumes of the layers involved in the
282 interaction with aroma compounds were expressed as products between compartment areas
283 and layer thicknesses (Eq. (A.12) to Eq. (A.16) in the Appendix A). Similarly to Doyennette
284 *et al.* (2014), transfer resistances on the air side ($1/k_{Oa}$, $1/k_{Fa}$ and $1/k_{Na}$) were assumed to be

285 negligible when compared to the transfer resistance on the wetted mucosa or saliva sides
286 ($1/k_{Om}$, $1/k_{Fm}$, $1/k_{Nm}$ and $1/k_{Os}$, $1/k_{Fs}$, respectively).

287 To improve the readability of the paper, only generic equations describing phenomena are
288 given in the text. They were written specifically for each compartment to obtain the complete
289 description of aroma release. The details of all model equations are given in the Appendix A.

290 3.2. Air flow rates

291 By convention, the air flow rates indicated in Figure 2 are positive if they follow the direction
292 of the arrow. With this convention, air flow rates in the different cavities Q_{Oa} , Q_{OFa} , Q_{Na} and
293 Q_{NFa} are positive (or null, depending on whether breathing occurs through the nose or the
294 mouth) during inhalation, and negative (or null) during exhalation. Conversely, air flow rate
295 from the trachea Q_{Ta} is negative during inhalation and positive during exhalation.

296 Air flow rate in the trachea due to breathing was assumed sinusoidal (Eq. (A.33)). According
297 to Figure 2 and to the experimental protocol, the air flow rate in the mouth is given by the
298 breathing flow rate during the first inhalation and is null afterwards (Eq. (A.34)). The opposite
299 was considered for the air flow rate in the nasal cavity (Eq. (A.35)). According to Figure 2,
300 the air balance in the pharynx at any time is given by the equality of inlet and outlet fluxes
301 (Eq. (A.36)).

302 3.3. Saliva in oral cavity

303 The volume of saliva in the oral cavity gradually increases due to the salivary flow rate Q_{Os}
304 and abruptly decreases after swallowing. A minimal residual volume of saliva V_{Osmin} was
305 assumed to remain in the mouth after swallowing (Doyennette *et al.*, 2014).

306 3.4. Mathematical description of interfacial conditions and fluxes

307 3.4.1. Air/mucosa and air /saliva interfaces

308 The interfacial aroma compound concentrations at air/mucosa or air/saliva interfaces were
309 obtained from the partition conditions at the interfaces, using the following generic equations:

310
$$C_{am}^*(t) = \frac{C_a(t)}{K_{am}}, \quad C_{as}^*(t) = \frac{C_a(t)}{K_{as}} \quad \text{Eq. 1}$$

311 Recall that transfer resistances on the air side were assumed negligible, hence, in the air,
 312 bulk and interfacial concentrations are identical. Specifically, the air/mucosa interfacial aroma
 313 compound concentrations are described by Eq. (A.17), Eq. (A.18) and Eq. (A.19) in oral,
 314 nasal or pharyngeal cavities, respectively. The air/saliva interfacial aroma compound
 315 concentrations are given by Eq. (A.20) and Eq. (A.21) in the oral or pharyngeal cavities,
 316 respectively.

317 Volatile mass fluxes ϕ_{am} and ϕ_{as} between the air and the other compartments (mucosa or
 318 saliva) are determined by the resistances located on the mucosa and saliva sides, respectively.
 319 They are given by the difference between the mucosa (C_m) or saliva (C_s) concentrations and
 320 the interfacial concentrations (C_{am}^*) or (C_{as}^*) and are calculated using the following generic
 321 equations:

322
$$\phi_{am} = k_m \times A_{am} \times (C_m(t) - C_{am}^*(t)), \quad \phi_{as} = k_s \times A_{as} \times (C_s(t) - C_{as}^*(t)) \quad \text{Eq. 2}$$

323 Specifically, in the oral cavity these fluxes are given by Eq. (A.26) and Eq. (A.29), in the
 324 pharynx by Eq. (A.28) and Eq. (A.30) and in the nose by Eq. (A.27).

325 3.4.2. Mucosa/saliva interface

326 Since the mucosa was assumed to be partially wetted by the saliva, aroma partition and flux
 327 between mucosa and saliva compartments was also considered in the oral and pharyngeal
 328 cavities. Transfer resistances were considered in both saliva and mucosa layers since they are
 329 expected to be of comparable magnitude. **Interfacial aroma compound concentrations at**
 330 **mucosa/saliva interface were obtained from the partition conditions at the interfaces, using the**
 331 **following generic equation (Figure 3):**

332
$$C_{sm}^*(t) = \frac{C_{ms}^*(t)}{K_{ms}} \quad \text{Eq. 3}$$

333 The mucosa/saliva interfacial aroma compound concentrations are described by Eq. (A.22)
 334 and Eq. (A.24) in oral or pharyngeal cavities, respectively. **The partition coefficients between**

335 mucosa and saliva were calculated based on partition coefficients with the air phase (Eq.
 336 (A.23) and Eq. (A.25)):

$$337 \quad K_{ms} = \frac{K_{as}}{K_{am}} \quad \text{Eq. 4}$$

338 Since the mucosa was assumed to be partially wetted by the saliva, a volatile flux between
 339 saliva and mucosa ϕ_{ms} was also considered (Eq. (A.31) in the oral cavity and Eq. (A.32) in
 340 the pharyngeal cavity):

$$341 \quad \phi_{ms}(t) = k_{eq} \times A_{ms} \times \left(C_s(t) - \frac{C_m(t)}{K_{ms}} \right) \quad \text{Eq. 5}$$

342 with k_{eq} being the equivalent mass transfer coefficients between saliva and wetted mucosa,
 343 with saliva taken as reference. It includes resistances in both phases in contact and the
 344 partition between them (Marin *et al.*, 1999):

$$345 \quad \frac{1}{k_{eq}} = \frac{1}{k_s} + \frac{K_{ms}}{k_m} \quad \text{Eq. 6}$$

346 3.5. Volatile mass balances

347 According to Figure 2, in each considered cavity the air may exchange aroma compounds
 348 with mucosa, saliva and air of connected cavities, as applicable. The generic volatile mass
 349 balance for the air in a cavity has the following form, where the term “source” denotes
 350 cavities which supply air to the cavity under consideration:

$$351 \quad V_a \frac{dC_a}{dt} = \phi_{am} + \phi_{as} + \sum_{source} Q_{a,source} (C_{a,source} - C_a) \quad \text{Eq. 7}$$

352 For the first inhalation, the variation of aroma concentration in the air in the oral cavity C_{Oa} is
 353 due to the volatile flux from the inhaled air sample and also to contact with the mucosa and
 354 saliva layers (Eq. (A.37)). For the following breathing cycles (through the nose), the mouth is
 355 closed (Eq. (A.38)). The mass balance in the air of the nasal cavity is given by Eq. (A.39),
 356 with no saliva layer present and the possible source of volatile compounds being the pharynx,
 357 during expiration. The pharynx has both saliva and mucosa layers and can exchange air with

358 the mouth (first inhalation) nose (subsequent breathing) and trachea, as described by Eq.
359 (A.40).

360 Saliva layers in mouth (Eq. (A.41)) and pharynx (Eq. (A.42)) exchange aroma compounds
361 with air and mucosa, according to the generic mass balance:

$$362 \quad V_s \frac{dC_{Fs}(t)}{dt} = -\phi_{as}(t) - \phi_{ms}(t) \quad \text{Eq. 8}$$

363 with the saliva in the oral cavity being additionally diluted by the fresh saliva flow rate.

364 Mucosa layers are in contact with air and saliva (except in the nose) and the mass balance for
365 these layers was written on the basis of Eq. 9 (developed as (Eq. A.43), (Eq. A.44) and (Eq.
366 A.45) in the oral, nasal and pharyngeal cavities, respectively):

$$367 \quad V_m \frac{dC_m(t)}{dt} = \phi_{ms}(t) - \phi_{am}(t) \quad \text{Eq. 9}$$

368 3.6. Reference values of the parameters

369 The reference values of parameters used for simulations are given in Table 4. Some were
370 taken from experimental data or from the literature, and were estimated when little
371 information was available. For instance, the contact area between air and mucosa in the nose
372 A_{Nam} was set to 150 cm² (Levitzky, 2003). Concerning air/mucosa partition properties, values
373 comprised between 5.6×10^{-5} and 4.8×10^{-1} were found for the air/mucus partition coefficient of
374 butanol and octanol in bullfrog (Hornung *et al.*, 1987). Thus, a typical reference value of
375 1×10^{-3} was selected in this case. Concerning the mucosa layer thickness, values between 500
376 and 800 μm in the mouth and 100 to 200 μm for the gingival mucosa were reported (Patel *et*
377 *al.*, 2012; Shojaei, 1998). It is expected, however, that aroma compounds will not necessarily
378 have time to diffuse in the whole epithelium thickness, so these values were considered as
379 upper limits for the mucosa layer thickness involved in aroma retention. That is why the
380 reference values for mucosa layer thicknesses in the present case in the different
381 compartments were fixed at 50 μm . On the basis of previous studies (Doyennette *et al.*, 2014),
382 the respiratory frequency F_R was set to 0.24 cycles per second. An analysis of model

383 sensitivity was done to determine the respective influence of each parameter on aroma release
384 kinetics.

385 3.7. Numerical methods

386 3.7.1. Solution of model equations

387 The dynamic model developed in this study consisted in nine coupled nonlinear differential
388 equations: eight for aroma compound concentrations in air, mucosa (oral, pharynx and nasal
389 cavities) and saliva (oral cavity and pharynx) plus one differential equation for saliva
390 accumulation in the oral cavity between swallowing events. Numeric calculations were
391 performed with Matlab® 8 software (The MathWorks Inc., Natick, MA). The variable step,
392 stiff ODE solver “ode15s” in the Matlab ODE suite (Shampine and Reichelt, 1997) was used
393 with both absolute and relative tolerances for all equations set to 10^{-8} . Integration step was
394 adjusted internally to meet the specified tolerances while results were provided at the required
395 (e.g. measurement) times. Integration was halted and restarted at each swallowing event to
396 allow abrupt changes in state variables, e.g. saliva volume decrease and air mixing in pharynx
397 related to the quick deglutition process (Doyennette *et al.*, 2014).

398 3.7.2. Sensitivity analysis

399 The model contains a total of 27 independent parameters (Table 4), i.e. which cannot be
400 calculated based on other ones (such as a volume being the product of an area and a layer
401 thickness). To assess the importance of these parameters for the prediction of the volatile
402 compound concentration in the nasal cavity (model output) a global Monte Carlo sensitivity
403 analysis was performed as follows. The model output was the relative volatile concentration
404 in the nasal cavity (C_{Na}^r), i.e. the predicted concentration (C_{Na}) of the aroma compound
405 divided by its maximum value. For a given value p_j of each parameter p , the relative local
406 sensitivity was defined as:

$$407 L(p_j) = \frac{1}{n_t} \sum_{i=1}^{n_t} \frac{|C_{Na}^r(t_i, p_j) - C_{Na}^r(t_i, p_j + \delta p)|}{|\delta p|} \times \frac{p_{ref}}{\max_{0 \leq t \leq 110} C_{Na}^r(t, p_{ref}) - \min_{0 \leq t \leq 110} C_{Na}^r(t, p_{ref})} \quad \text{Eq. (10)}$$

408 where $C_{Na}^r(t_i, p_j)$ is the output of the model calculated for time $t_i \in [0, 110]$ s with the
409 considered parameter value set to p_j and δp is a perturbation of the parameter, taken as 10%
410 of its minimum value indicated in Table 4. Thus $L(p_j)$ represents an approximation of the
411 partial derivative of the nasal concentration with respect to the considered parameter, taken in
412 absolute value and averaged over time. To make sensitivities dimensionless, of order of unity
413 and hence comparable among various parameters, the right-hand side scaling factor was
414 introduced, based on the reference value of the parameter given in Table 4.

415 The global sensitivity of a parameter was calculated as an average of local sensitivities across
416 a large number of samples taken in the parametric space:

$$417 \quad G(p) = \frac{1}{1000} \sum_{j=1}^{1000} L(p_j) \quad \text{Eq. (11)}$$

418 The parametric space was defined by the range of variation of each parameter indicated in
419 Table 4 and sampled according to a multidimensional “Latin hypercube” method to ensure a
420 uniform representation of all parameter values. Parameters whose range of variation spanned
421 more than one order of magnitude were evenly sampled on a logarithmic rather than linear
422 scale.

423 Automatic sensitivity analysis gives global information on the relative importance of various
424 parameters for the nasal concentration prediction, but provides little insight in the involved
425 phenomena. A manual sensitivity analysis was also performed by varying some of the
426 parameters (specified in the results section) one by one while keeping the others at their
427 reference values. Parameters whose possible variation range was large (sometimes several
428 orders of magnitude) were included in the manual sensitivity analysis, while those relatively
429 well known from the experimental protocol and physiological measurements were kept
430 constant.

431 3.7.3. Model fitting

432 To test the ability of the model to reproduce release curves observed for different molecules,
433 some of the least well known parameters were estimated based on release data. The number of
434 estimated parameters was kept at a minimum, however. Volumes, contact areas, respiratory
435 frequency and deglutition times were either known from physiological measurements or
436 imposed by the experimental protocol; these parameters were kept fixed to their reference
437 values indicated in Table 4. Partition coefficients between air and saliva ($K_{Oas} = K_{Fas}$) were
438 experimentally determined for the three aroma compounds; these values were used without
439 change. The estimated parameters, assumed to be the same in all cavities, were the transfer
440 coefficient in the saliva ($k_{Os} = k_{Fs}$, the same for all molecules) because *in vivo* hydrodynamic
441 conditions are poorly known, and parameters related to the mucosa layer: thickness ($e_{Om} =$
442 $e_{Fm} = e_{Nm}$, common to all molecules), transfer coefficient ($k_{Om} = k_{Fm} = k_{Nm}$, also
443 common to all molecules) and air/mucosa partition coefficients ($K_{Oam} = K_{Fam} = K_{Nam}$),
444 expected to vary strongly with the physico-chemical properties of the studied compounds and
445 hence specific to each molecule.

446 Model fitting was thus performed simultaneously using data from release experiments with
447 the three molecules, the partition coefficients being specific to each molecule but common to
448 all cavities and the other abovementioned parameters common to all molecules and all
449 cavities. The fitting criterion was the sum of the absolute values of the errors between model
450 predictions and experimental measurements of the compound concentration in the nasal
451 cavity, both normalised by their respective maximum values (C_{Na}^*), because measured data
452 was only available in arbitrary units. Since possible ranges of some of the parameters span up
453 to 4 orders of magnitude (Table 4) a “global” optimisation procedure based on genetic
454 programming was used, namely the “ga” implementation in the Matlab® Global Optimization
455 Toolbox, with default settings (e.g. population of 40 individuals, convergence tolerance 10^{-6})
456 and the maximum number of generations increased to 200. Parameters whose search range

457 (Table 4) spanned more than one order of magnitude were sampled on a logarithmic scale, i.e.
458 the logarithm of the parameter was actually searched for by the optimisation algorithm. Since
459 the considered optimisation algorithm is stochastic, several (~10) optimisation runs were
460 performed and the one with the best fit was selected. Consistent convergence to similar values
461 of the parameters (usually within $\pm 15\%$) was observed in most runs.

462 4. Results and discussion

463 4.1. Molecule specific effects on aroma release kinetics

464 As previously highlighted (Dél ris *et al.*, 2015), significant differences between aroma
465 compounds in terms of release descriptors were observed (Figure 4).

466 Differences in $I_{\max 1}$ and $I_{\max 2}$ and in AUC_1 and AUC_2 were explained by differences in
467 inhaled gaseous concentrations of molecules due to different aqueous concentrations and
468 air/water partition properties. They were thus not shown nor discussed here.

469 Before swallowing (Figure 4-a), no difference between molecules was observed concerning
470 t_{\max} . Yet, the peak width $\Delta t_{20\%_1}$ of 2-nonanone was the largest and those of ethyl propanoate
471 the narrowest. After swallowing, differences in release behaviours were more pronounced
472 since some temporal parameters were significantly different between molecules: ethyl
473 propanoate was released the most rapidly and with a quite narrow peak, whereas (Z)-3-hexen-
474 1-ol had the most delayed release, with the largest peak at 50% of I_{\max} ($t_{50\%}-t_{\max}$), and
475 2-nonanone had the largest peak at 20% of I_{\max} ($\Delta t_{20\%_2}$) (Figure 4-b). Initial release rates were
476 molecule-dependent both before and after swallowing (Figure 4-c). Ethyl propanoate was
477 released faster than (Z)-3-hexen-1-ol (before and after swallowing) and 2-nonanone (only
478 before swallowing).

479 AUC_{stand} , which can be associated with molecule persistence, also reflected differences in
480 release behaviour: the highest value was obtained for 2-nonanone, highlighting quite
481 persistent release behaviour for this molecule (Figure 4-d). In contrast, ethyl propanoate

482 presented the lowest values of AUC_{stand} . The AUC_1/AUC_2 ratios were higher than 1 for all
483 molecules, meaning that a greater amount was released before swallowing than after.
484 However, a 30-fold increase in AUC_1/AUC_2 ratio was observed between 2-nonanone and
485 ethyl propanoate, meaning that the latter was mainly released before swallowing, whereas
486 2-nonanone was released during both phases.

487 All these results were in agreement with previous observations and confirmed the probable
488 existence of retention phenomena for some aroma compounds. To get insight in the exact
489 nature of these interactions, notably in the respective roles of the physicochemical properties
490 of the molecules, of saliva and/or of mucosa characteristics, model simulations and sensitivity
491 analysis were used.

492 We could also mention that from these results, no clear relationship between aroma release
493 and anatomical or physiological parameters was observed

494 4.2. Simulations of aroma compound release kinetics

495 One of the advantages of using a modelling approach is the possible determination of the time
496 variation of variables that could not be experimentally determined, providing insight in the
497 involved mechanisms. Examples of simulated release kinetics obtained with the model in the
498 different compartments of the naso-oro-pharyngeal cavities are presented in Figure 5.

499 As a starting point, model parameters were fixed to their reference values, determined either
500 from data in the literature or experimentally (Table 4). Air/mucosa contact areas in the mouth
501 A_{Oam} and in the pharynx A_{Fam} were fixed at 10% of the total area of the mouth A_{O} and the
502 pharynx A_{F} , respectively, meaning that 90% of the mouth and pharynx surfaces were wetted
503 by saliva. The resulting kinetics were considered as a reference. The inset on each figure
504 illustrates the first 3 seconds of the release to better understand initial phenomena. Just after
505 sample inhalation through the mouth, the gaseous concentrations of aroma compounds in the
506 pharynx C_{Fa} and in the mouth C_{Oa} increased (Figures 5-a and 5-d, respectively). In parallel,

507 molecules accumulated within mucosa and saliva layers both in the mouth (Figures 5-e and 5-
508 f, respectively) and in the pharynx (Figures 5-b and 5-c, respectively). When the mouth was
509 closed (at 2 s), aroma compound gaseous concentration in the air in the mouth started to
510 decrease, as well as in the pharynx. In the mouth, the slow decrease in the gaseous
511 concentration of aroma compounds after 2s was due to adsorption on mucosa and saliva
512 layers. In the pharynx, the expiration flow rate accounts for the much faster decrease since it
513 was responsible for the transport of aroma compounds from the pharynx to the nose (increase
514 in aroma compound concentration in the nose C_{Na} (Figure 5-g) and, therefore, a decrease in
515 aroma compound concentration in the pharynx C_{Fa} (Figure 5-a). The adsorption of aroma
516 compounds on mucosa is also probably involved in this decrease. The pulse in aroma
517 concentration in the nasal cavity led to an increase in aroma concentration within the nasal
518 mucosa layer C_{Nm} (Figure 5-h). Yet, aroma compound concentration in the nose air rapidly
519 decreased to zero since air from the lungs was aroma-free and the aroma transfer from the
520 nasal mucosa to the air in the nose (which occurred as aroma concentration in the nasal
521 mucosa progressively decreased; Figure 5-h) was not rapid enough to compensate for the
522 dilution by the breath flow rate. Similar conclusions can be drawn concerning the variation of
523 concentrations in pharynx compartments.

524 The first swallow occurred at 20 s. It led to a sudden decrease in saliva volume in the mouth
525 V_{Os} (Figure 5-i), as well as decreases in aroma compound concentrations in the air within the
526 mouth (C_{Oa} , Figure 5-d) and in saliva in the mouth C_{Os} (Figure 5-f) and in the pharynx C_{Fs}
527 (Figure 5-c). In all mucosa compartments, concentrations C_{Fm} , C_{Om} and C_{Nm} progressively
528 decreased, highlighting the unloading of these compartments (Figures 5-b, 5-e and 5-h,
529 respectively). These mass transfers were probably the limiting steps since aroma
530 concentrations in the different air phases C_{Fa} , C_{Oa} and C_{Na} did not increase (Figures 5-a, 5-d
531 and 5-g, respectively). The saliva volume in the mouth followed a cyclic variation, with a

532 linear increase due to the saliva flow rate between each swallowing event and a sudden
533 decrease when swallowing occurred.

534 4.3. Sensitivity analysis of the model to physicochemical and physiological parameters

535 Modelling makes it possible to easily test the effect of parameters that govern mass transfers,
536 notably those that cannot be modified when performing *in vivo* studies. Such a sensitivity
537 analysis can contribute to the determination of the nature of the key factors underlying aroma
538 release and persistence.

539 4.3.1. Global sensitivity analysis

540 Based on the results of the global sensitivity analysis performed as described in section
541 3.7.2, model parameters were arbitrarily divided in three groups, according to their influence
542 on the shape of the nasal concentration release curve (recall that nasal concentration was
543 always normalized by its maximum value). The first group included 3 most influential
544 parameters, with global relative sensitivities comprised between 0.4 and 0.2: the air/mucosa
545 partition coefficients in the nose (K_{Nam}) and in the pharynx (K_{Fam}) and the respiratory
546 frequency (F_{R}). The second group included 5 moderately influential parameters, with
547 sensitivities between 0.1 and 0.025: air/mucosa partition coefficient in the mouth (K_{Oam}),
548 air/saliva partition coefficient in the mouth (K_{Oas}) and pharynx (K_{Fas}), mass transfer
549 coefficient in the mouth (k_{Os}) and the tidal volume (V_{C}). The other parameters listed in Table
550 4 had sensitivities less than 0.025.

551 Overall, these results support the central assumption underlying this work, namely that in
552 absence of any food product, volatile persistence in consumer's exhaled air is mainly related
553 to the interaction between the aroma compound and subject's mucosa, quantified in the model
554 via the air/mucosa partition coefficients. A second important factor, already pointed out in
555 presence of non masticated (Tréléa *et al.*, 2008) and masticated (Doyennette *et al.*, 2014) food
556 products, is the consumer's breath via the respiratory frequency and current breath volume.

557 Mass transfer and geometry (volumes, contact areas) appear to play a smaller role in volatile
558 persistence than in release from food products.

559 4.3.2. Manual sensitivity analysis

560 When dealing with mass transfer, the main factors governing molecule transports are the
561 contact area, the driving force (dependent, in particular, on the partition properties of the
562 molecules) and the mass transfer coefficient of the molecules. Simulations were thus
563 performed to evaluate their influence on release kinetics. The ranges of variation of model
564 parameter values were chosen to be in agreement with physicochemical or physiological
565 values (Table 4). Only the effects of these modifications on the simulated release kinetics in
566 the nasal cavity are explained since they correspond to what can be experimentally
567 determined. The variation of aroma concentrations in other compartments were simulated but
568 are not discussed here.

569 First, to better understand the respective roles of the saliva and mucosa compartments, some
570 simulations were performed without any saliva compartment (air/mucosa contact areas in the
571 mouth and in the pharynx were equal to the total surfaces of the mouth and the pharynx,
572 respectively, so contact areas with saliva were equal to zero, Table 4) .

573 The absence of saliva as well as the modification of mucosa thickness (10-fold variation
574 factor) did not have an impact on the shape of release kinetics of aroma compounds within the
575 nasal cavity. Differences were mainly observed on mucosa concentration and unloading rates
576 (not shown). For example, mucosa concentrations in the mouth and in the pharynx were 5 to
577 9-fold higher, respectively, without saliva than with saliva, and 10-fold higher or lower when
578 the thickness decreased or increased, respectively. Mucosa compartments also unloaded more
579 rapidly when saliva was not considered or when mucosa thicknesses were lower.

580 The mass transfer coefficient of aroma compounds in mucosa had a greater impact on the
581 release kinetics in the nasal cavity when it increased than when it decreased (not shown).

582 With an increased mass transfer coefficient in mucosa, mucosa loading and unloading rates
583 were higher. Since air flow rate remained constant between simulations, mucosa
584 compartments were more rapidly unloaded and the gaseous concentration in the nose was thus
585 lower and decreased more rapidly. The effects with decreased values of mass transfer
586 coefficients were less obvious: below a value of 10^{-6} m/s, very slow aroma transport prevents
587 any significant amount of aroma compound to be loaded into the mucosa, so there is almost
588 no impact on aroma concentration in the nose.

589 Decreasing the air/mucosa partition properties had a big impact on the nasal concentration of
590 aroma compounds and the shape of release kinetics. A low air/mucosa partition means high
591 affinity of the aroma compound for the mucosa compartment. Most of the aroma compound
592 was thus retained within the mucosa and released very slowly in tiny amounts according to
593 breathing cycles. Persistence was thus long but the actual concentration in the nasal cavity
594 was low. A 100-fold increase in the air/mucosa partition from 10^{-3} had less effect on the
595 aroma concentration in the nose than a 100-fold decrease, due to the fact that the amounts of
596 aroma compound loaded into the mucosa became negligible.

597 These results revealed which parameters related to mucosa had an impact on release kinetics.
598 However, except in the nasal cavity, mucosa is always wetted by a saliva film. Mucosa
599 parameters were thus fixed to their reference values and saliva parameters were modified to
600 evaluate their influence on aroma release kinetics. As a reference, it was assumed that saliva
601 covered 90% of the mouth and pharynx surfaces.

602 Simulations were performed by increasing this percentage up to 100% without any significant
603 effect (not shown). When saliva is considered, mucosa concentrations are lower due to: (i) the
604 reduced contact area between air and mucosa and, consequently, lower loading rates of
605 mucosa compartments in the mouth and in the pharynx; and (ii) the fact that part of the aroma

606 compound was captured by saliva instead of mucosa. Nevertheless, there was no impact on
607 nasal concentration and release kinetics.

608 100-fold variations in the mass transfer coefficients of molecules in saliva did not affect
609 release kinetics in the nasal cavity (not shown). The only consequences were modifications of
610 aroma concentrations in saliva.

611 Concerning the modifications of air/saliva partition properties, only a 100-fold decrease
612 significantly modified release kinetics as a consequence of a higher affinity of aroma
613 compounds for saliva. Saliva becomes the main aroma reservoir, supplying aroma compounds
614 to the air in the nasal cavity until the first swallow at 20 s. Aroma concentrations increased in
615 saliva (50-fold and 60-fold factors in the pharynx and the mouth, respectively) and decreased
616 in mucosa (6-fold and 3-fold factors in the pharynx and the mouth, respectively) (not shown).

617 Simulations were also performed by varying mouth and pharynx volumes and the salivary
618 flow rate (in the range of experimental values, determined on panellists), but no significant
619 difference was obtained between simulations (not shown), **confirming the absence of effect of**
620 **these parameters in the range of variation that was tested.**

621 On the basis of these results, it can be concluded that both saliva and mucosa had an impact
622 on aroma release when the affinity of aroma compounds for these compartments was
623 sufficiently high. Mechanistic modelling provided insight into the relative time distributions
624 of the aroma compound among these compartments.

625 4.4. Adjustment of simulated release kinetics to experimental data

626 To validate model assumptions, model simulations were fitted to experimental data. Three
627 experimental kinetics were used, each one representing specific release behaviour (related to
628 specific aroma compounds). Several parameters were used as degrees of freedom: the
629 effective mucosa thickness participating to aroma retention, the mass transfer coefficients of
630 aroma compounds in saliva and in mucosa and the air/mucosa partition coefficients of aroma

631 compounds. For these parameters, values were assumed to be the same in all physiological
632 cavities (mouth, pharynx and nose).

633 Figures 6-a, 6-b and 6-c indicate the good fit that was obtained between experimental
634 (1 panellist, 1 replicate) and simulated release kinetics of ethyl propanoate, (Z)-3-hexen-1-ol
635 and 2-nonanone, respectively.

636 Concerning fitted parameters, the final value of mucosa thickness **was modified (26 μm) but**
637 **remained in a realistic order of magnitude.** In a first approach, it was set at a similar value for
638 all physiological cavities (nose, pharynx and mouth) since sensitivity analysis did not show a
639 significant influence of this parameter on release kinetic shape. For further studies, it could
640 perhaps be interesting to more accurately study the impact of this parameter since the nose,
641 mouth and pharynx mucosa are clearly physiologically different.

642 The values of the mass transfer coefficients of aroma compounds **reached 6.0×10^{-5} m/s in**
643 **saliva and 4.9×10^{-5} m/s in mucosa.** They were on the order of magnitude of the one used as a
644 reference for simulations and were the same for the three molecules. This result is in
645 agreement with the fact that these coefficients mainly depend on the hydrodynamics in the
646 system and little on molecule properties (Marin *et al.*, 1999). The fact that the mass transfer
647 coefficient in saliva was higher than the one in mucosa was quite expected and can be
648 explained by the difference in viscosity between saliva and mucus. Yet, the absolute values of
649 these mass transfer coefficients in mucosa and saliva were quite high in comparison with the
650 data in the literature (3×10^{-6} m/s) (Marin *et al.*, 1999). The high degree of mixing that
651 probably exists in the naso-oro-pharyngeal cavities can account for this discrepancy (the data
652 in the literature were related to *in vitro* studies).

653 The air/mucosa partition properties of aroma compounds ranged **between 4.7×10^{-4} (2-**
654 **nonanone) and 6.9×10^{-3} (ethyl propanoate),** the one of (Z)-3-hexen-1-ol being intermediate. In
655 the case of ethyl propanoate, the air/**mucosa** partition coefficient increased by a **factor of 7**

656 compared to reference values, so that the model correctly predicted the experimental release
657 kinetics. It thus appeared that this molecule has limited interaction with saliva and mucosa.
658 The shape of release kinetics in this case is therefore mainly explained by the pulse of the
659 aroma compound due to sample inhalation and air renewal in the mouth at swallowing (Figure
660 6-a). Concerning 2-nonanone, the 2-fold decrease in the air/mucosa partition value suggests
661 that 2-nonanone interacts more with mucosa than the other two compounds. For (Z)-3-hexen-
662 1-ol, the value of air/mucosa partition properties after model fitting was only slightly
663 modified in comparison to the reference values and remained thus in the same order of
664 magnitude than the air/saliva partition coefficient.

665 On the basis of these results, we could argue that both air/mucosa and air/saliva partition
666 properties are, at least partly, at the origin of the release behaviours that were observed for the
667 molecules: the ones with the lower affinity for saliva and/or mucosa (highest partition
668 coefficients) had the least persistent behaviour.

669 All these results confirmed that *in vivo* release behaviours were strongly molecule-dependent
670 and highlighted the fact that different types of interactions with mucosa and/or saliva were
671 involved, depending on the molecule's properties. These simulations were in agreement with
672 previous experimental data, which notably showed the limited retention of ethyl propanoate
673 and the specific retention of 2-nonanone in the oral and pharyngeal cavities (Déléris *et al.*,
674 2015). To improve simulations, further development of the model could be foreseen, notably
675 concerning assumptions on mucosa. This will require experimental determination of mucosa
676 properties.

677 5. Conclusions

678 In conclusion, it appears that the proposed model adequately simulated aroma release and
679 retention after the inhalation of a gaseous flavoured sample by panellists. The simulation of
680 the time variation of concentrations that cannot be determined experimentally helped to better

681 understand the involved phenomena. The sensitivity analysis contributed to distinguish the
682 respective roles of saliva and mucosa on aroma retention phenomena. **No clear effect of cavity**
683 **volumes or saliva flow rate on aroma release kinetics was highlighted in the range of variation**
684 **of parameters that was tested. But results confirmed the particular role of wetted mucosa can**
685 **play, depending on aroma compound properties.** This study constitutes a first step in
686 understanding aroma persistence and further work is needed to clarify the relationships
687 between the properties of molecules and the type of interactions that are involved.

688 6. Appendix A: model equations

	Oral cavity	Nasal cavity	Pharynx
Volumes			
wetted mucosa	Eq. (A.12) $V_{Om} = e_{Om} \times A_{Oam}$	Eq. (A.13) $V_{Nm} = e_{Nm} \times A_{Nam}$	Eq. (A.14) $V_{Fm} = e_{Fm} \times A_{Fam}$
saliva	Eq. (A.15) $V_{Os} = e_{Os} \times A_{Oas}$	n. a.	Eq. (A.16) $V_{Fs} = e_{Fs} \times A_{Fas}$
Interfacial concentrations			
air/mucosa	Eq. (A.17) $C_{Oam}^*(t) = \frac{C_{Oa}(t)}{K_{Oam}}$	Eq. (A.18) $C_{Nam}^*(t) = \frac{C_{Na}(t)}{K_{Nam}}$	Eq. (A.19) $C_{Fam}^*(t) = \frac{C_{Fa}(t)}{K_{Fam}}$
air/saliva	Eq. (A.20) $C_{Oas}^*(t) = \frac{C_{Oa}(t)}{K_{Oas}}$	n. a.	Eq. (A.21) $C_{Fas}^*(t) = \frac{C_{Fa}(t)}{K_{Fas}}$
mucosa/saliva	Eq. (A.22) $C_{Osm}^*(t) = \frac{C_{Oms}^*(t)}{K_{Oms}}$ Eq. (A.23) $K_{Oms} = \frac{K_{Oas}}{K_{Oam}}$	n. a.	Eq. (A.24) $C_{Fsm}^*(t) = \frac{C_{Fms}^*(t)}{K_{Fms}}$ Eq. (A.25) $K_{Fms} = \frac{K_{Fas}}{K_{Fam}}$
Volatile mass fluxes			
air/mucosa	Eq. (A.26) $\phi_{Oam}(t) = k_{Om} \times A_{Oam} \times (C_{Om}(t) - C_{Oam}^*(t))$	Eq. (A.27) $\phi_{Nam}(t) = k_{Nm} \times A_{Nam} \times (C_{Nm}(t) - C_{Nam}^*(t))$	Eq. (A.28) $\phi_{Fam}(t) = k_{Fm} \times A_{Fam} \times (C_{Fm}(t) - C_{Fam}^*(t))$
air/saliva	Eq. (A.29) $\phi_{Oas}(t) = k_{Os} \times A_{Oas} \times (C_{Os}(t) - C_{Oas}^*(t))$		Eq. (A.30) $\phi_{Fas}(t) = k_{Fs} \times A_{Fas} \times (C_{Fs}(t) - C_{Fas}^*(t))$
mucosa/saliva	Eq. (A.31) $\phi_{Oms}(t) = k_{Oeq} \times A_{Oms} \times (C_{Os}(t) - \frac{C_{Om}(t)}{K_{Oms}})$		Eq. (A.32) $\phi_{Fms}(t) = k_{Feq} \times A_{Fms} \times (C_{Fs}(t) - \frac{C_{Fm}(t)}{K_{Fms}})$
Air flow rates			
breathing	Eq. (A.33) $Q_{Ta}(t) = -\pi \times F_R \times Vc \times \sin(2 \times \pi \times F_R \times t)$		
	Eq. (A.34) $Q_{Oa}(t) = Q_{OFa}(t) =$ $\begin{cases} -Q_{Ta}(t) & \text{if } t \leq 1/(2 \times F_R) \text{ (1st inhalation)} \\ 0 & \text{if } t > 1/(2 \times F_R) \text{ (breathing through the nose)} \end{cases}$	Eq. (A.35) $Q_{Na}(t) = Q_{NFa}(t) =$ $\begin{cases} 0 & \text{if } t \leq 1/(2 \times F_R) \text{ (1st inhalation)} \\ -Q_{Ta} & \text{if } t > 1/(2 \times F_R) \text{ (breathing through the nose)} \end{cases}$	Eq. (A.36) $Q_{OFa}(t) + Q_{NFa}(t) = -Q_{Ta}(t)$
Volatile mass balances			
air	Eq. (A.37) $V_{Oa} \times \frac{dC_{Oa}(t)}{dt} = \phi_{Oam}(t) + \phi_{Oas}(t) + Q_{Oa}(t) \times C_{ext}(t) - Q_{OFa} \times C_{Oa}(t)$ for $t \leq 1/(2 \times F_R)$ (1st inhalation) Eq. (A.38) $V_{Oa} \times \frac{dC_{Oa}(t)}{dt} = \phi_{Oam}(t) + \phi_{Oas}(t)$ for $t > 1/(2 \times F_R)$ (other breathing cycles, through the nose)	Eq. (A.39) $V_{Na} \times \frac{dC_{Na}(t)}{dt} = \phi_{Nam}(t) - \begin{cases} Q_{NFa}(t) \times C_{Fa}(t) - Q_{Na}(t) \times C_{Na}(t) & \text{if } Q_{Ta}(t) \geq 0 \text{ (expiration)} \\ Q_{NFa}(t) \times C_{Na}(t) & \text{if } Q_{Ta}(t) < 0 \text{ (inspiration)} \end{cases}$	Eq. (A.40) $V_{Fa} \times \frac{dC_{Fa}(t)}{dt} = \phi_{Fam}(t) + \phi_{Fas}(t) + \begin{cases} Q_{OFa}(t) \times C_{Oa}(t) + Q_{Ta}(t) \times C_{Fa}(t) & \text{if } t \leq 1/(2 \times F_R) \text{ (1st inhalation)} \\ Q_{NFa}(t) \times C_{Fa}(t) & \text{if } t > 1/(2 \times F_R) \text{ and } Q_{Ta}(t) \geq 0 \text{ (expiration)} \\ Q_{NFa}(t) \times C_{Na}(t) + Q_{Ta}(t) \times C_{Fa}(t) & \text{if } t > 1/(2 \times F_R) \text{ and } Q_{Ta}(t) < 0 \text{ (inspiration)} \end{cases}$
saliva	Eq. (A.41) $V_{Os} \times \frac{dC_{Os}(t)}{dt} = -(\phi_{Oas}(t) + \phi_{Oms}(t) + Q_{Os} \times C_{Os}(t))$	n. a.	Eq. (A.42) $V_{Fs} \times \frac{dC_{Fs}(t)}{dt} = -\phi_{Fas}(t) - \phi_{Fms}(t)$
mucosa	(Eq. A.43) $V_{Om} \times \frac{dC_{Om}(t)}{dt} = \phi_{Oms}(t) - \phi_{Oam}(t)$	(Eq. A.44) $V_{Nm} \times \frac{dC_{Nm}(t)}{dt} = -\phi_{Nam}(t)$	(Eq. A.45) $V_{Fm} \times \frac{dC_{Fm}(t)}{dt} = \phi_{Fms}(t) - \phi_{Fam}(t)$

689 n. a.: not applicable

690 7. Acknowledgments

691 We gratefully acknowledge the panellists for their contribution to *in vivo* and sensory
692 measurements. We also thank Gilles Feron from UMR 1324 INRA/AgroSup
693 Dijon/CNRS/Université de Bourgogne Centre des Sciences du Goût et de l'Alimentation
694 (CSGA) for the characterisation of saliva samples, and Gail Wagman for revising the English
695 version of the manuscript.

696 8. References

- 697 Anker, L., Jurs, P.C., Edwards, P.A., (1990). Quantitative structure-retention relationship
698 studies of odor-active aliphatic compounds with oxygen-containing functional groups.
699 *Analytical Chemistry*, 62(24), 2676-2684.
- 700 Barron, D., Pineau, N., Matthey-Doret, W., Ali, S., Sudre, J., Germain, J.C., Kolodziejczyk,
701 E., Pollien, P., Labbe, D., Jarisch, C., Dugas, V., Hartmann, C., Folmer, B., (2012). Impact of
702 crema on the aroma release and the in-mouth sensory perception of espresso coffee. *Food &*
703 *Function*, 3(9), 923-930.
- 704 Benjamin, O., Silcock, P., Beauchamp, J., Buettner, A., Everett, D.W., (2012). Tongue
705 Pressure and Oral Conditions Affect Volatile Release from Liquid Systems in a Model
706 Mouth. *Journal of Agricultural and Food Chemistry*, 60(39), 9918-9927.
- 707 Biasioli, F., Gasperi, F., Aprea, E., Endrizzi, I., Framondino, V., Marini, F., Mott, D., Mark,
708 T., (2006). Correlation of PTR-MS spectral fingerprints with sensory characterisation of
709 flavour and odour profile of "Trentingrana" cheese. *Food Quality and Preference*, 17(1-2),
710 63-75.
- 711 Borysik, A.J., Briand, L., Taylor, A.J., Scottt, I.M., (2010). Rapid Odorant Release in
712 Mammalian Odour Binding Proteins Facilitates Their Temporal Coupling to Odorant Signals.
713 *Journal of Molecular Biology*, 404(3), 372-380.

714 Buettner, A., Beauchamp, J., (2010). Chemical input – Sensory output: Diverse modes of
715 physiology–flavour interaction. *Food Quality and Preferences*, 21(8), 915-924.

716 Buettner, A., Mestres, M., (2005). Investigation of the Retronasal Perception of Strawberry
717 Aroma Aftersmell Depending on Matrix Composition. *Journal of Agricultural and Food*
718 *Chemistry*, 53(5), 1661-1669.

719 Buffo, R.A., Rapp, J.A., Krick, T., Reineccius, G.A., (2005). Persistence of aroma compounds
720 in human breath after consuming an aqueous model aroma mixture. *Food Chemistry*, 89(1),
721 103-108.

722 Chastrette, M., Rallet, E., (1998). Structure-minty odour relationships: Suggestion of an
723 interaction pattern. *Flavour and Fragrance Journal*, 13(1), 5-18.

724 Corley, R.A., Kabilan, S., Kuprat, A.P., Carson, J.P., Minard, K.R., Jacob, R.E., Timchalk,
725 C., Glenny, R., Pipavath, S., Cox, T., Wallis, C.D., Larson, R.F., Fanucchi, M.V.,
726 Postlethwait, E.M., Einstein, D.R., (2012). Comparative Computational Modeling of Airflows
727 and Vapor Dosimetry in the Respiratory Tracts of Rat, Monkey, and Human. *Toxicological*
728 *Sciences*, 128(2), 500-516.

729 Cussler, E.L., (1997). *Diffusion. Mass Transfer in Fluid Systems*. (2ème édition ed).
730 University Press, Cambridge.

731 Déléris, I., Kauffmann, M., Saint Eve, A., Féron, G., Souchon, I., (2015). Experimental
732 approaches to better understand the retention of aroma compounds in oro-naso-pharyngeal
733 cavities in: Buettner, A., Beauchamp, J., Guthrie, B., Lavine, B.K. (Eds.), *The Chemical*
734 *Sensory Informatics of Food: Measurement, Analysis, Integration*, Washington DC.

735 Déléris, I., Saint Eve, A., Dakowski, F., Sémon, E., Le Quéré, J.L., Souchon, I., (2011). The
736 dynamics of aroma release during the consumption of candies with different structures.
737 Relationship with temporal perception. *Food Chemistry*, 127, 1615-1624.

738 Doyennette, M., De Loubens, C., Déléris, I., Souchon, I., Tréléa, I.C., (2011). Mechanisms
739 explaining the role of viscosity and post-deglutitive pharyngeal residue on in vivo aroma
740 release: A combined experimental and modeling study *Food Chemistry*, 128(2), 380-390.

741 Doyennette, M., Déléris, I., Féron, G., Guichard, E., Souchon, I., Tréléa, I.C., (2014). Main
742 individual and product characteristics influencing in-mouth flavour release during eating
743 masticated food products with different textures: mechanistic modelling and experimental
744 validation. *Journal of theoretical biology*, 340, 209-221.

745 Espinosa Diaz, M., (2004). Comparison between orthonasal and retronasal flavour perception
746 at different concentrations. *Flavour and Fragrance Journal*, 19(6), 499-504.

747 Féron, G., Ayed, C., Qannari, E.M., Courcoux, P., Labouré, H., Guichard, E., (2014).
748 Understanding Aroma Release from Model Cheeses by a Statistical Multiblock Approach on
749 Oral Processing. *Plos One*, 9(4), e93113.

750 Ferreira, V., Petka, J., Cacho, J., (2006). Intensity and persistence profiles of flavor
751 compounds in synthetic solutions. Simple model for explaining the intensity and persistence
752 of their aftersmell. *Journal of Agricultural and Food Chemistry*, 54(2), 489-496.

753 Foster, K.D., Grigor, J.M.V., Cheong, J.N., Yoo, M.J.Y., Bronlund, J.E., Morgenstern, M.P.,
754 (2011). The Role of Oral Processing in Dynamic Sensory Perception. *Journal of Food*
755 *Science*, 76(2), R49-R61.

756 Frank, D.C., Eyres, G.T., Piyasiri, U., Delahunty, C.M., (2012). Effect of food matrix
757 structure and composition on aroma release during oral processing using *in vivo* monitoring.
758 *Flavour and Fragrance Journal*, 27(6), 433-444.

759 Geerts, T., Heyden, Y.V., (2011). In Silico Predictions of ADME-Tox Properties: Drug
760 Absorption. *Combinatorial Chemistry & High Throughput Screening*, 14(5), 339-361.

761 Gierczynski, I., Guichard, E., Labouré, H., (2011). Aroma perception in dairy products: the
762 roles of texture, aroma release and consumer physiology. A review. *Flavour and Fragrance*
763 *Journal*, 26(3), 141-152.

764 Halpern, B.P., (2004). Retronasal and orthonasal smelling. *ChemoSens*, 6(3), 1-7.

765 Harrison, M., (2000). Mathematical models of release and transport of flavors from foods in
766 the mouth to the olfactory epithelium, in: Roberts, D.D., Taylors, A.J. (Eds.), *Flavor Release*,
767 Washington, DC, pp. 179-191.

768 Harrison, M., Hills, B.P., (1997). Mathematical model of flavor release from liquids
769 containing aroma-binding macromolecules. *Journal of Agricultural and Food Chemistry*, 45,
770 1883-1890.

771 Heath, M.R., (2002). The oral management of food: the bases of oral success and for
772 understanding the sensations that drive us to eat. *Food Quality and Preference*, 13(7-8), 453-
773 461.

774 Heenan, S., Soukoulis, C., Silcock, P., Fabris, A., Apréa, E., Cappellin, L., Gasperi, F.,
775 Biasioli, F., (2011). PTR-TOF-MS monitoring of *in vitro* and *in vivo* flavour release in cereal
776 bars with varying sugar composition. *Food Chemistry*, 131(2), 477-484.

777 Heenan, S.P., Dufour, J.P., Hamid, N., Harvey, W., Delahunty, C.M., (2009).
778 Characterization of fresh bread flavour: Relationships between sensory characteristics and
779 volatile composition. *Food Chemistry*, 116(1), 249-257.

780 Heilman, S., Hummel, T., (2004). A new method for comparing orthonasal and retronasal
781 olfaction. *Behavioral Neuroscience*, 118, 412-419.

782 Hodgson, M., Parker, A., Linforth, R.S.T., Taylor, A.J., (2004). *In vivo* studies on the long
783 term persistence of volatiles in the breath. *Flavour and Fragrance Journal*, 19(6), 470-475.

784 Hodgson, M.D., Langridge, J.P., Linforth, R.S.T., Taylor, A.J., (2005). Aroma release and
785 delivery following the consumption of beverages. *Journal of Agricultural and Food*
786 *Chemistry*, 53(5), 1700-1706.

787 Hornung, D.E., Youngentob, S.L., Mozell, M.M., (1987). Olfactory Mucosa-Air Partitioning
788 of Odorants. *Brain Research Bulletin*, 413(1), 147-154.

789 Hummel, T., (2008). Retronasal perception of odors. *chemistry and biodiversity*, 5(6), 853-
790 861.

791 Hummel, T., Heilmann, S., Landis, B.N., Reden, J., Frasnelli, J., Small, D.M., Gerber, J.,
792 (2006). Perceptual differences between chemical stimuli presented through the ortho- or
793 retronasal route. *Flavour and Fragrance Journal*, 21(1), 42-47.

794 Keyhani, K., Scherer, P.W., Mozell, M.M., (1997). A numerical model of nasal odorant
795 transport for the analysis of human olfaction. *Journal of theoretical biology*, 186(3), 279-301.

796 Kraft, P., Bajgrowicz, J.A., Denis, C., Frater, G., (2000). Odds and trends: Recent
797 developments in the chemistry of odorants,. *Angewandte Chemie International Edition*, 17,
798 2981-3010.

799 Kurtz, D.B., Zhao, K., Hornung, D.E., Scherer, P., (2004). Experimental and numerical
800 determination of odorant solubility in nasal and olfactory mucosa. *Chemical Senses*, 29(9),
801 763-773.

802 Levitzky, M.G., (2003). *Pulmonary physiology*. McGraw-Hill Companies Inc., USA.

803 Marin, M., Baek, I., Taylor, A.J., (1999). Volatile release from aqueous solutions under
804 dynamic headspace dilution conditions. *Journal of Agricultural and Food Chemistry*, 47(11),
805 4750-4755.

806 Martin-Harris, B., (2006). Coordination of respiration and swallowing, *GI Motility online*
807 www.nature.com.

808 Medinsky, M.A., Kimbell, J.S., Morris, J.B., Gerde, P., Overton, J.H., (1993). Advances in
809 biologically based models for respiratory-tract uptake of inhaled volatiles. *Fundamental and*
810 *applied toxicology*, 20(3), 265-272.

811 Morris, J.B., (2012). Biologically-based modeling insights in inhaled vapor absorption and
812 dosimetry. *Pharmacology & Therapeutics*, 136(3), 401-413.

813 Neyraud, E., Palicki, O., Schwartz, C., Nicklaus, S., Peron, G., (2012). Variability of human
814 saliva composition: Possible relationships with fat perception and liking. *Archives of Oral*
815 *Biology*, 57(5), 556-566.

816 Normand, V., Avison, S., Parker, A., (2004). Modeling the Kinetics of Flavour Release during
817 Drinking. *Chemical Senses*, 29(3), 235-245.

818 Obata, K., Sugano, K., Saitoh, R., Higashida, A., Nabuchi, Y., Machida, M., Aso, Y., (2005).
819 Prediction of oral drug absorption in humans by theoretical passive absorption model.
820 *International Journal of Pharmaceutics*, 293(1-2), 183-192.

821 Patel, V.F., Liu, F., Brown, M.B., (2012). Modeling the oral cavity: In vitro and in vivo
822 evaluations of buccal drug delivery systems. *journal of controlled release*, 161(3), 746-756.

823 Repoux, M., Laboure, H., Courcoux, P., Andriot, I., Semon, E., Yven, C., Feron, G.,
824 Guichard, E., (2012a). Combined effect of cheese characteristics and food oral processing on
825 in vivo aroma release. *Flavour and Fragrance Journal*, 27(6), 414-423.

826 Repoux, M., Sémon, E., Féron, G., Guichard, E., Labouré, H., (2012b). Inter-individual
827 variability in aroma release during sweet mint consumption. *Flavour and Fragrance Journal*,
828 27, 40-46.

829 Rognon, C., Chastrette, M., (1994). Structure-odor relationships - a highly predictive
830 tridimensional interaction-model for the bell-pepper note. *European Journal of medicinal*
831 *chemistry*, 29(7-8), 595-609.

832 Sanz, G., Thomas-Danguin, T., Hamdani, E.H., Le Poupon, C., Briand, L., Pernollet, J.C.,
833 Guichard, E., Tromelin, A., (2008). Relationships between molecular structure and perceived
834 odor quality of ligands for a human olfactory receptor. *Chemical Senses*, 33(7), 639-653.

835 Shampine, L.F., Reichelt, M.W., (1997). The MATLAB ODE Suite. *SIAM Journal on*
836 *Scientific Computing*, 18, 1-22.

837 Sherwood, L., (2006). *Fundamentals of physiology: a human perspective*. Thomson
838 Brooks/cole, Belmont, USA.

839 Shojaei, A.H., (1998). Buccal mucosa as a route for systemic drug delivery: a review. *Journal*
840 *of Pharmaceutical Sciences*, 1(1), 15-30.

841 Sun, B.C., Halpern, B.P., (2005). Identification of air phase retronasal and orthonasal odorant
842 pairs. *Chemical Senses*, 30(8), 693-706.

843 Takano, R., Sugano, K., Higashida, A., Hayashi, Y., Machida, M., Aso, Y., Yamashita, S.,
844 (2006). Oral absorption of poorly water-soluble drugs: Computer simulation of fraction
845 absorbed in humans from a miniscale dissolution test. *Pharmaceutical Research*, 23(6), 1144-
846 1156.

847 Tortora, G.J., Anagnostakos, N.P., (1990). *Principles of anatomy and physiology* Harper-
848 Collins, New-York.

849 Tréléa, I.C., Atlan, S., Déléris, I., Saint-Eve, A., Marin, M., Souchon, I., (2008). Mechanistic
850 mathematical model for in vivo aroma release during eating of semi-liquid foods. *Chemical*
851 *Senses*, 33(2), 181-192.

852 Tromelin, A., Merabtine, Y., Andriot, I., Lubbers, S., Guichard, E., (2010). Retention-release
853 equilibrium of aroma compounds in polysaccharide gels: Study by quantitative structure-
854 activity/property relationships approach. *Flavour and Fragrance Journal*, 25(6), 431.

855 Visschers, R.W., Jacobs, M.A., Frasnelli, J., Hummel, T., Burgering, M., Boelrijk, A.E.M.,
856 (2006). Cross-Modality of Texture and Aroma Perception Is Independent of Orthonasal or
857 Retronasal Stimulation. *Journal of Agricultural and Food Chemistry*, 51(14), 5509-5515.

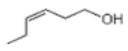
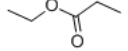
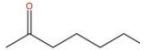
858 Weel, K.G.C., Boelrijk, A.E.M., Alting, A.C., Van Mil, P.J.J.M., Burrows, H.D., Gruppen,
859 H., Voragen, A.G.J., Smit, G., (2002). Flavor Release and Perception of Flavored Whey
860 Protein Gels: Perception Is Determined by Texture Rather than by Release. *Journal of*
861 *Agricultural and Food Chemistry*, 50(18), 5149-5155.

862 Welge-Lüssen, A., Ebnöther, M., Wolfensberger, M., Hummel, T., (2009). Swallowing Is
863 Differentially Influenced by Retronasal Compared with Orthonasal Stimulation in
864 Combination with Gustatory Stimuli. *Chemical Senses*, 34, 499-502.

865 Wright, K.M., Hills, B.P., (2003). Modelling flavour release from a chewed bolus in the
866 mouth: Part II. The release kinetics. *International Journal of Food Science and Technology*,
867 38(3), 361-368.

868 Yabuki, M., Scott, D.J., Briand, L., Taylor, A.J., (2011). Dynamics of Odorant Binding to
869 Thin Aqueous Films of Rat-OBP3. *Chemical Senses*, 36(7), 659-671.

870 Table 1: Physicochemical properties of aroma compounds used in the present study.

<i>Aroma compounds</i>	<i>Chemical formulae</i>	<i>Chemical structures</i>	<i>Molecular weights (g/mol)</i>	<i>Log P¹</i>	<i>PTR-MS² fragmentation: main m/z peaks (relative abundance)</i>	<i>Air/water partition coefficient (25°C)¹</i>	<i>Experimental air/water partition coefficient K_{aw} (×10⁻³) (37°C)³</i>	<i>Experimental air/saliva partition coefficient K_{as} (×10⁻³) (37°C)³</i>
(Z)-3-Hexen-1-ol	C ₆ H ₁₂ O		100.16	1.61	55 (100); 83 (39)	0.63 10 ⁻³	0.78 ± 0.07	0.76 ± 0.12
Ethyl propanoate	C ₅ H ₁₀ O ₂		102.13	1.21	75 (100); 103 (20)	15.9 10 ⁻³	14.9 ± 1.4	12.9 ± 5.5
2-Nonanone	C ₉ H ₁₈ O		142.24	3.14	143 (100); 41 (20)	11.1 10 ⁻³	19.6 ± 8.4	9.7 ± 1.39

871 ¹: estimation with EPI SuiteTM programme872 ²: PTR-MS: Proton Transfer Reaction-Mass Spectrometry873 ³: from (Dél  ris *et al.*, 2015)

874 Table 2: Minimal, median and maximal values of the physiological characteristics of
 875 panellists and associated quartiles.

	Physiological parameters	min	Q1	median	Q3	max
Salivary parameters at rest	V _C (L)	0.49	0.54	0.80	0.86	0.93
	V _{nose} (cm ³)	5.8	9.5	11.1	13.1	16.8
	V _{mouth} (cm ³)	33.1	35.5	39.3	56.7	69.8
	V _{pharynx} (cm ³)	16.8	24.3	27.4	30.2	34.8
	Salivary flux (g/min)	0.32	0.44	0.54	0.66	0.87
	Antioxidant (eq mM Trolox)	75.4	90.7	105.7	127.5	137.3
	Lipolysis (mU/mL)	0.04	0.08	0.15	0.19	0.27
	Amylase (U/mL)	67.4	88.7	124.8	148.6	196.0
	Proteolysis (U/mL)	1.6	1.9	4.1	4.8	11.2
	Lysozyme (U/mL)	313.2	332.2	413.9	444.1	462.1
	Proteins (mg/mL)	0.46	0.55	0.81	0.94	1.15

876

877 Table 3: Definition of model variables

Symbol	Unit	Definition
C_{Fa}	g/cm^3	Aroma concentration in the air in the pharynx
C_{Fm}	g/cm^3	Aroma concentration in the wetted mucosa in the pharynx
C_{Fs}	g/cm^3	Aroma concentration in saliva in the pharynx
C_{Fam}^*	g/cm^3	Aroma concentration at the air/wetted mucosa interface in the pharynx
C_{Fas}^*	g/cm^3	Aroma concentration at the air/saliva interface in the pharynx
C_{Fms}^*	g/cm^3	Aroma concentration at the wetted mucosa/saliva interface in the pharynx, on the mucosa side
C_{Fsm}^*	g/cm^3	Aroma concentration at the wetted mucosa/saliva interface in the pharynx, on the saliva side
C_{Oa}	g/cm^3	Aroma concentration in the air in the oral cavity
C_{Om}	g/cm^3	Aroma concentration in the wetted mucosa in the oral cavity
C_{Os}	g/cm^3	Aroma concentration in saliva in the oral cavity
C_{Oam}^*	g/cm^3	Aroma concentration at the air/wetted mucosa interface in the oral cavity
C_{Oas}^*	g/cm^3	Aroma concentration at the air/saliva interface in the oral cavity
C_{Oms}^*	g/cm^3	Aroma concentration at the wetted mucosa/saliva interface in the oral cavity, on the mucosa side
C_{Osm}^*	g/cm^3	Aroma concentration at the wetted mucosa/saliva interface in the oral cavity, on the saliva side
C_{Na}	g/cm^3	Aroma concentration in the air in the nose
C_{Nm}	g/cm^3	Aroma concentration in the mucosa in the nose
C_{Nam}^*	g/cm^3	Aroma concentration at the air/mucosa interface in the nose
C_{Ta}	g/cm^3	Aroma concentration in the trachea
Q_{Na}	cm^3/s	Air flow rate into the nasal cavity
Q_{NFa}	cm^3/s	Air flow rate from the nasal cavity to the pharynx
Q_{Oa}	cm^3/s	Air flow rate into the oral cavity (1 st inhalation)
Q_{OFa}	cm^3/s	Air flow rate from the oral cavity to the pharynx
Q_{Ta}	cm^3/s	Air flow rate from the trachea
t	s	Time
t_{deg}	s	Swallowing moment
ϕ_{Fam}	g/s	Volatile mass flux between the air and the wetted mucosa in the pharynx
ϕ_{Fas}	g/s	Volatile mass flux between the air and the saliva in the pharynx
ϕ_{Fms}	g/s	Volatile mass flux between the wetted mucosa and the saliva in the pharynx
ϕ_{Nam}	g/s	Volatile mass flux between the air and mucosa in the nasal cavity
ϕ_{Oam}	g/s	Volatile mass flux between the air and the wetted mucosa in the oral cavity
ϕ_{Oas}	g/s	Volatile mass flux between the air and the saliva in the oral cavity
ϕ_{Oms}	g/s	Volatile mass flux between the wetted mucosa and the saliva in the oral cavity

878 Table 4: Definition, reference values and range of variations used for simulations of model
879 parameters.

Symbol	Unit	Definition	Reference value	Range of variation	Global sensitivity index (from Monte-Carlo analysis) ^a	Source
A_F	cm ²	Total area of the pharynx	65	32.5 ... 130	+	(Doyennette <i>et al.</i> , 2014)
A_{Fam}	cm ²	Air/mucosa contact area in pharynx	$= 0.1 \times A_F$	$0.1 \times A_F - A_F$	+	-
A_{Fas}	cm ²	Air/saliva contact area in pharynx	$= A_F - A_{Fam}$	/	+	-
A_{Fms}	cm ²	Mucosa/saliva contact area in pharynx	$= A_F - A_{Fam}$	/	+	-
A_{Nam}	cm ²	Air/mucosa contact area in nose	150	75 ... 300	+	(Levitzky, 2003)
A_O	cm ²	Total area in oral cavity	116	58 ... 232	+	(Doyennette <i>et al.</i> , 2014)
A_{Oam}	cm ²	Air/mucosa contact area in oral cavity	$= 0.1 \times A_O$	$0.1 \times A_O - A_O$	+	-
A_{Oas}	cm ²	Air/saliva contact area in oral cavity	$= A_O - A_{Oam}$	/	+	-
A_{Oms}	cm ²	Mucosa/saliva contact area in oral cavity	$= A_O - A_{Oam}$	/	+	-
C_{ext}	µg/cm ³	Aroma concentration in air	1	0.5 ... 2	+	Experimental value
e_{Fm}	cm	Thickness of wetted mucosa in pharynx	$5 \cdot 10^{-3}$	$5 \cdot 10^{-4} \dots 5 \cdot 10^{-2}$	+	(Shojaei, 1998)
e_{Fs}	cm	Thickness of saliva layer in pharynx	$= V_{Fs}/A_{Fas}$	-	/	-
e_{Om}	cm	Thickness of wetted mucosa in oral cavity	$5 \cdot 10^{-3}$	$5 \cdot 10^{-4} \dots 5 \cdot 10^{-2}$	+	(Shojaei, 1998)
e_{Os}	cm	Thickness of saliva layer in oral cavity	$= V_{Os}/A_{Oas}$	/	/	-
e_{Nm}	cm	Thickness of mucosa in nasal cavity	$5 \cdot 10^{-3}$	$5 \cdot 10^{-4} \dots 5 \cdot 10^{-2}$	+	(Shojaei, 1998)
F_R	Cycle/s	Respiratory frequency	0.24	0.12 ... 0.48	+++	(Doyennette <i>et al.</i> , 2014)
K_{Fam}		Air/wetted mucosa partition coefficient in pharynx	10^{-3}	$10^{-5} \dots 10^{-1}$	+++	(Hornung <i>et al.</i> , 1987)
K_{Fas}		Air/saliva partition coefficient in pharynx	$5 \cdot 10^{-3}$	$5 \cdot 10^{-4} \dots 5 \cdot 10^{-2}$	++	Experimental values
K_{Fms}		Wetted mucosa/saliva partition coefficient in pharynx	$= K_{Fas}/K_{Fam}$	/	/	-
K_{Nam}		Air/ mucosa partition coefficient in nasal cavity	10^{-3}	$10^{-5} \dots 10^{-1}$	+++	(Hornung <i>et al.</i> , 1987)
K_{Oam}		Air/wetted mucosa partition coefficient in oral cavity	10^{-3}	$10^{-5} \dots 10^{-1}$	++	(Hornung <i>et al.</i> , 1987)
K_{Oas}		Air/saliva partition coefficient in oral cavity	$5 \cdot 10^{-3}$	$5 \cdot 10^{-4} \dots 5 \cdot 10^{-2}$	++	Experimental values
K_{Oms}		Wetted mucosa/saliva partition coefficient in oral cavity	$= K_{Oas}/K_{Oam}$	/	/	-
k_{Fa}	m/s	Mass transfer coefficient in air in pharynx	10^{-2}	/	/	(Cussler, 1997)
k_{Fm}	m/s	Mass transfer coefficient in wetted mucosa in pharynx	10^{-6}	$10^{-8} \dots 10^{-4}$	+	(Cussler, 1997)
k_{Fs}	m/s	Mass transfer coefficient in saliva in pharynx	10^{-6}	$10^{-8} \dots 10^{-4}$	+	(Cussler, 1997)
k_{Feq}	m/s	Equivalent mass transfer coefficient between saliva and wetted mucosa in pharynx	$1/k_{Feq} = 1/k_{Fs} + K_{Fms}/k_{Fm}$	/	/	(Marin <i>et al.</i> , 1999)
k_{Na}	m/s	Mass transfer coefficient in air in nasal cavity	10^{-2}	/	/	(Cussler, 1997)
k_{Nm}	m/s	Mass transfer coefficient in mucosa in nasal cavity	10^{-6}	$10^{-8} \dots 10^{-4}$	+	(Cussler, 1997)
k_{Oa}	m/s	Mass transfer coefficient in air in the oral cavity	10^{-6}	/	/	(Cussler, 1997)
k_{Om}	m/s	Mass transfer coefficient in wetted mucosa in the oral cavity	10^{-6}	$10^{-8} \dots 10^{-4}$	+	(Cussler, 1997)
k_{Os}	m/s	Mass transfer coefficient in saliva in oral cavity	10^{-6}	$10^{-8} \dots 10^{-4}$	++	(Cussler, 1997)
k_{Oeq}	m/s	Equivalent mass transfer coefficient between saliva and wetted mucosa in oral cavity	$1/k_{Oeq} = 1/k_{Os} + K_{Oms}/k_{Om}$	/	/	(Marin <i>et al.</i> , 1999)
Q_{Os}	cm ³ /s	Average rate of saliva flow rate	0.6	0.15 ... 2.4	+	Experimental values
t_{deg}	s	Swallowing moment	20, 50, 80, 110	/	/	Defined by the experimental protocol
V_C	cm ³	Current breath volume	800	400 ... 1600	++	Experimental values
V_{Fa}	cm ³	Volume of air in the pharynx	30	15 ... 60	+	Experimental values
V_{Fm}	cm ³	Volume of wetted mucosa in pharynx	$= e_{Fm} \times A_{Fam}$	/	/	-
V_{Fs}	cm ³	Volume of saliva in pharynx	0.2	0.1 ... 0.4	+	-
V_{Na}	cm ³	Volume of air in nasal cavity	20	10 ... 40	+	-

V_{Nm}	cm^3	Volume of mucosa in nasal cavity	$=e_{Nm} \times A_{Nam}$	/	/	-
V_{Oa}	cm^3	Volume of air in oral cavity	40	20 ... 80	+	Experimental value
V_{Om}	cm^3	Volume of wetted mucosa in oral cavity	$=e_{Om} \times A_{Oam}$	/	/	-
V_{Os}	cm^3	Volume of saliva in oral cavity	$=e_{Os} \times A_{Oas}$	/	/	-
V_{Osmin}	cm^3	Minimal volume of saliva in oral cavity after swallowing	0.2	0.1 ... 0.4	+	(Doyennette <i>et al.</i> , 2014)

880

881 ^a Global sensitivity index: +++ means a highly influent parameter (sensitivity index between
882 0.4 and 0.2); ++ means a moderately influent parameter (sensitivity index between 0.1 and
883 0.025); + was used for parameters with sensitivity index below 0.025.

Figure captions

Fig. 1: Schematic representation of the experimental set-up for the preparation of gaseous samples with controlled volume.

Fig. 2: Schematic representation of the interconnected compartments of the naso-oro-pharyngeal cavities and the mechanisms involved in aroma release during the inhalation of gaseous samples.

Fig. 3: Schematic representation of the balances between the different compartments. Bold red lines represent concentration profiles and horizontal dotted lines represent the limits of boundary layers where mass transfer resistance was considered.

Fig. 4: Comparison of parameters extracted from release kinetics that significantly differ between ions (**means and associated standard deviations**). (a) $t_{\max 1}$ and $\Delta t_{20\%_1}$, before swallowing; (b) $t_{\max 2}$, $\Delta t_{20\%_2}$ and $t_{50\%} - t_{\max 2}$, after swallowing; (c) initial release rates Rate_1 and Rate_2 ; (d) $\text{AUC}_1/\text{AUC}_2$ ratio and $\text{AUC}_{\text{stand}}$. Significant differences were determined using Kruskal-Wallis tests and the Conover-Iman procedure ($p < 0.05$) and highlighted with letters a to c.

Fig. 5: Simulated release kinetics using the model with the reference values of the parameters (Table 4): variation over time of aroma compound concentrations in (a) the air phase within the pharynx; (b) the mucosa layer in the pharynx; (c) saliva in the pharynx; (d) the air phase in the mouth; (e) the mucosa layer in the mouth; (f) saliva in the mouth; (g) the air phase in the nose; (h) the mucosa layer in the nose; and (i) the variation over time of saliva volume in the mouth. For each figure (except i), the insets focus on the first 3 seconds.

Fig. 6: Comparison between individual experimental and simulated release kinetics of: (a) ethyl propanoate (m/z 75); (b) (*Z*)-3-hexenol (m/z 83); and (c) 2-nonanone (m/z 143) in the nasal cavity. Experimental release kinetics were obtained by PTR-MS measurements during

the inhalation of gaseous sample by one panellist. d) Values of the parameters that were changed for model fitting (with respect to reference values).

Figure 1

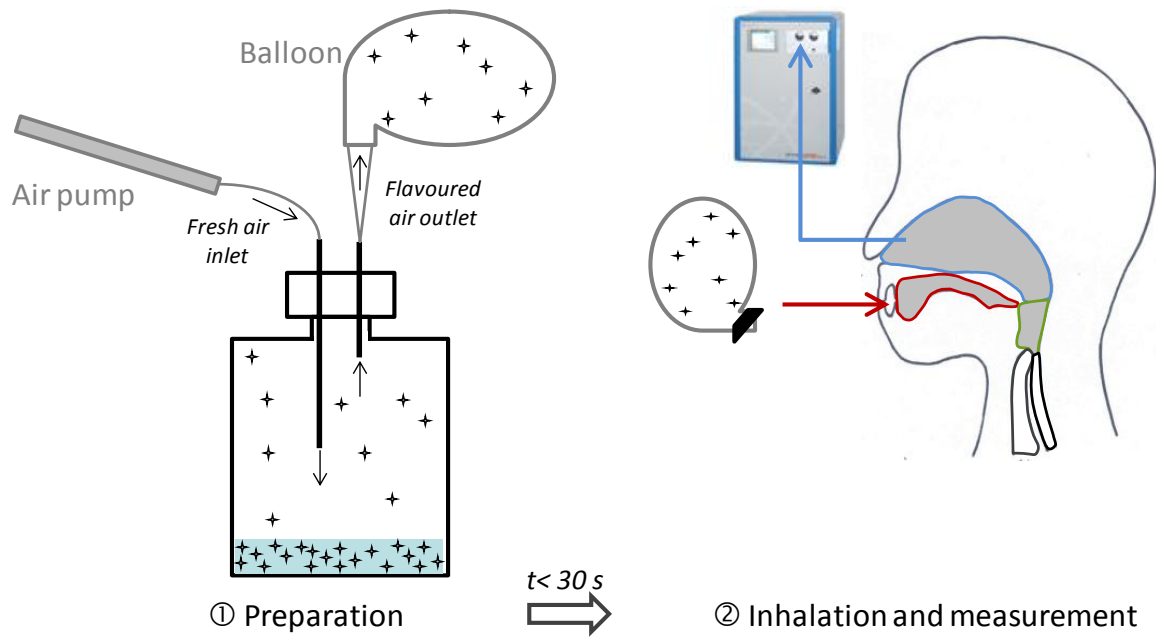


Figure 1. Schematic representation of the experimental set-up for the preparation of gaseous samples with controlled volume.

Figure2

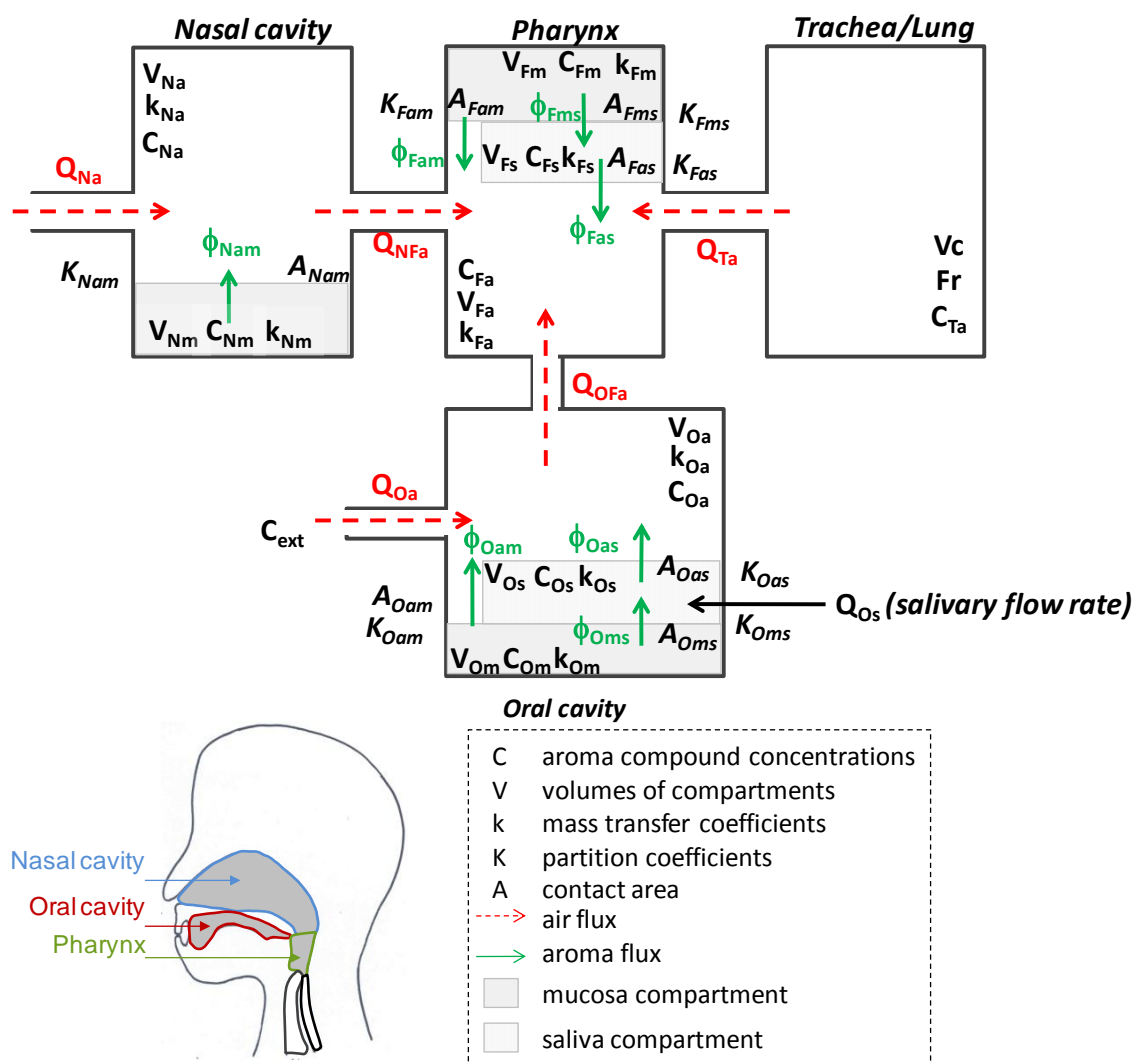


Figure 2. Schematic representation of the interconnected compartments of the naso-oro-pharyngeal cavities and the mechanisms involved in aroma release during the inhalation of gaseous samples.

Figure3

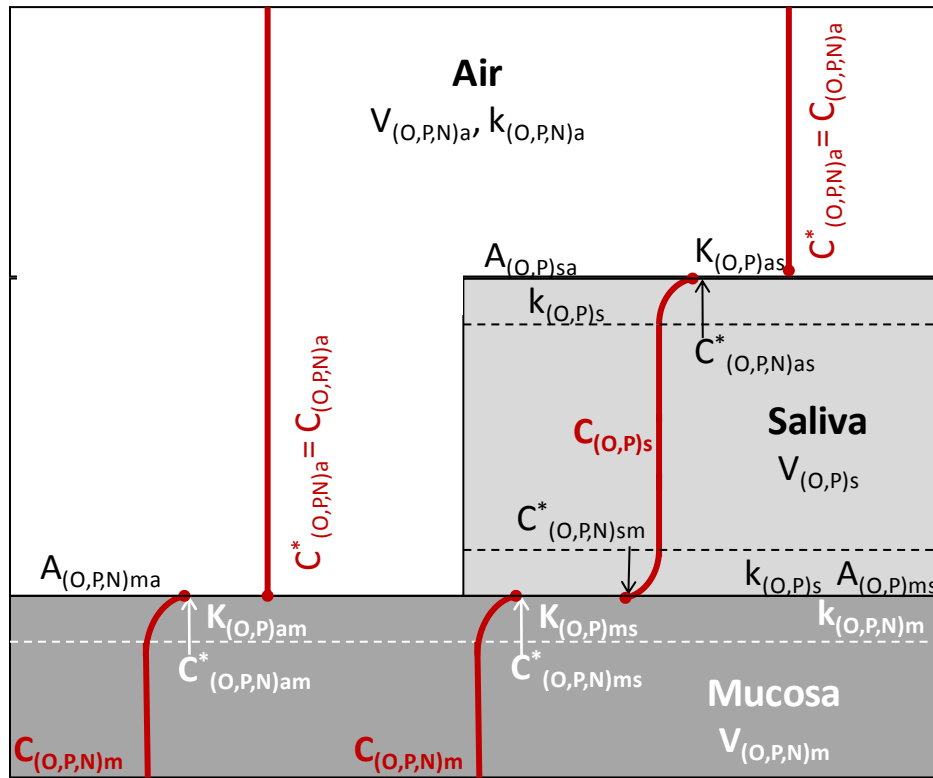


Figure 3. Schematic representation of the balances between the different compartments. Bold red lines represent concentration profiles and horizontal dotted lines represent the limits of boundary layers where mass transfer resistance was considered.

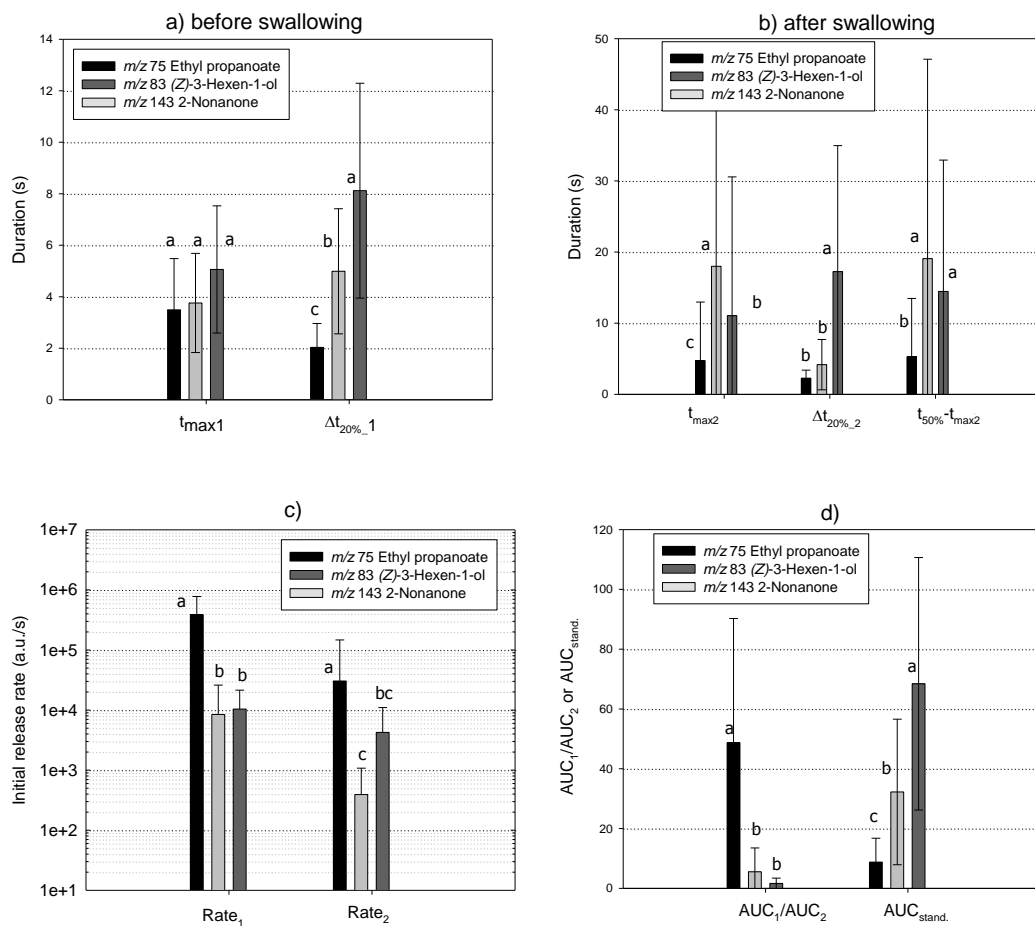


Figure 4. Comparison of parameters extracted from release kinetics that significantly differ between ions (means and associated standard deviations). (a) $t_{\max 1}$ and $\Delta t_{20\%_1}$, before swallowing; (b) $t_{\max 2}$, $\Delta t_{20\%_2}$ and $t_{50\%} - t_{\max 2}$, after swallowing; (c) initial release rates $Rate_1$ and $Rate_2$; (d) AUC_1/AUC_2 ratio and $AUC_{stand.}$ Significant differences were determined using Kruskal-Wallis tests and the Conover-Iman procedure ($p < 0.05$) and highlighted with letters a to c.

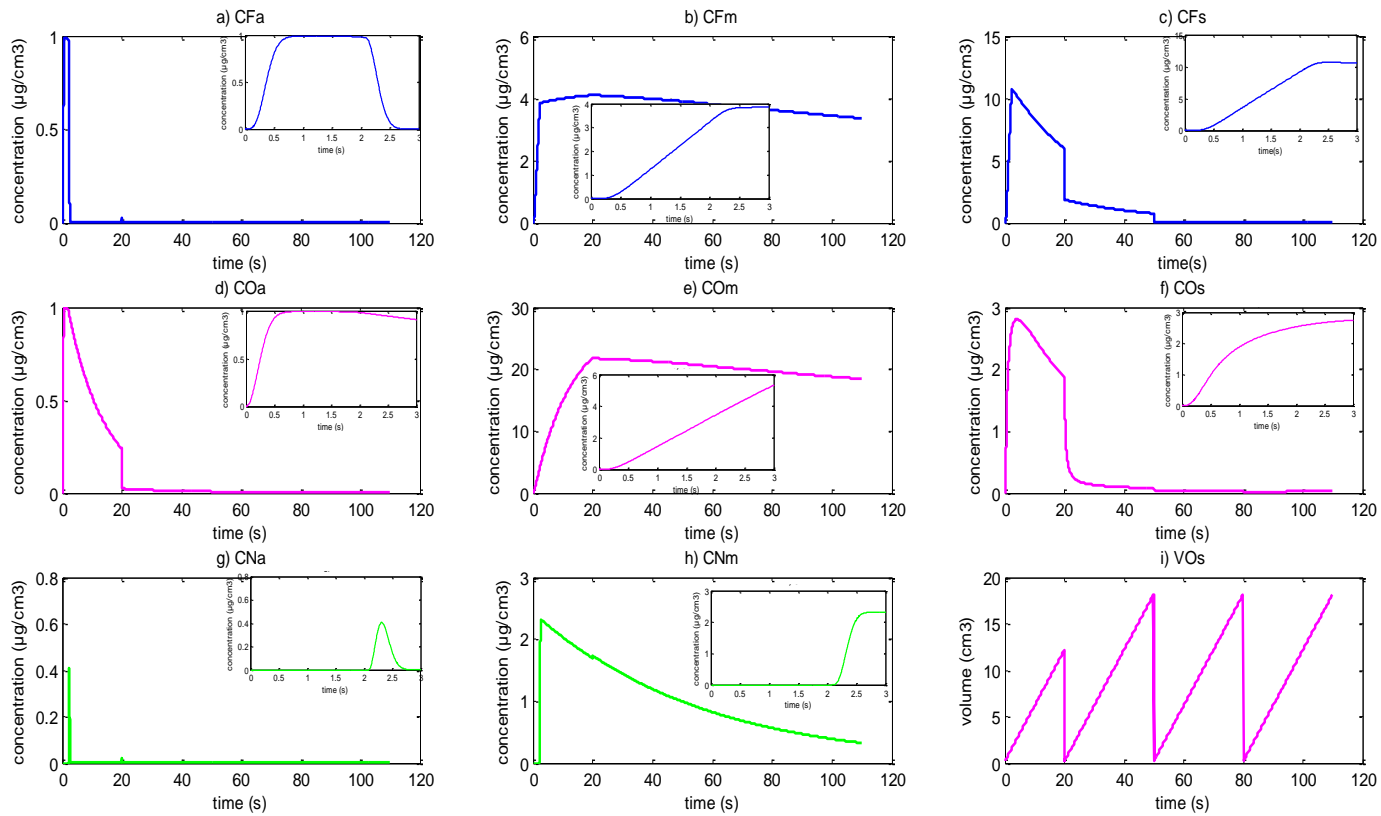


Figure 5. Simulated release kinetics using the model with the reference values of the parameters (Table 4): variation over time of aroma compound concentrations in (a) the air phase within the pharynx; (b) the mucosa layer in the pharynx; (c) saliva in the pharynx; (d) the air phase in the mouth; (e) the mucosa layer in the mouth; (f) saliva in the mouth; (g) the air phase in the nose; (h) the mucosa layer in the nose; and (i) the variation over time of saliva volume in the mouth. For each figure (except i), the insets focus on the first 3 seconds.

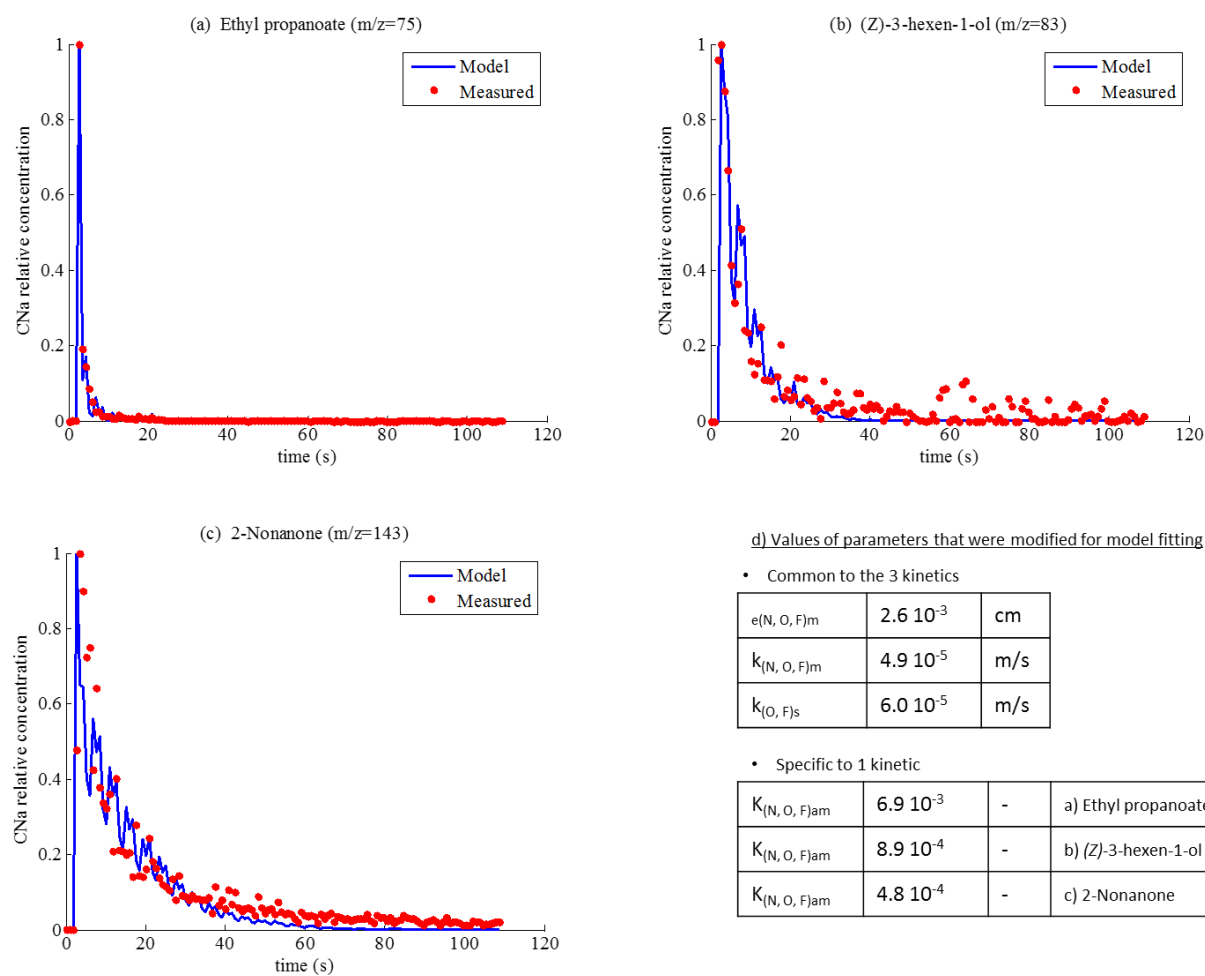


Figure 6. Comparison between individual experimental and simulated release kinetics of: (a) ethyl propanoate (m/z 75); (b) (Z)-3-hexenol (m/z 83); and (c) 2-nonanone (m/z 143) in the nasal cavity. Experimental release kinetics were obtained by PTR-MS measurements during the inhalation of gaseous sample by one panellist using the NMS protocol. d) Values of the parameters that were changed for model fitting (with respect to reference values).